



MASTER THESIS

STUDIES ON THE ELECTROCHEMICAL REDUCTION OF CARBONDIOXIDE AND NITRITE

Supervisor at TU Wien:

*Ao.Univ.Prof. Dipl.-Ing. Dr.techn. Fafilek Günter
Institute of Chemical Technologies and Analytics*

Supervisor at UCLA:

*Assistant Professor Carlos Morales-Guio
Samueli School of Engineering*

Maximilian Winzely, BSc.

01611158

May, 2021

Acknowledgment

At the beginning I want to thank the Marshall Plan Foundation, the TU Wien for the "KUWI-Stipend" and the Industriellenvereinigung Kärnten for financially supporting my stay at the UCLA.

Of course, a special thanks goes to Ass. Prof. Carlos Morales-Guio for his exceptional supervision of my master thesis and his ambitious character which has motivated me very much during my research work.

Further, I would like to thank Joonbaek Jang (aka the korean lord), not only one of my colleagues but also a special friend who made my work in the lab and my time in Los Angeles unforgettable even during a pandemic.

I would like to thank Prof. Günter Faflek who was very helpful during my stay and supported me when necessary.

Another thank you goes to my friends in Los Angeles, especially Renée, for the wonderful and also unforgettable time where I hope for many reunions in the future.

And in the end I would like to thank my mother for her cheerful calls and tireless support in all my decisions, who never wanted to accept that her son has to work in academia even on weekends.

Abstract

In recent years the topic climate change has been becoming increasingly important and the need of solutions for decreasing use of fossil fuels and reduction of greenhouse gases such as carbon dioxide in the atmosphere is more and more urgent. The introduction of new technologies in the near future is unavoidable as global warming is proceeding at an unprecedented rate. Renewable energy sources such as solar power or wind power must be made more cost-effective and the storage of the electricity generated must be improved.

In this work the electrochemical reduction of carbon dioxide (CO_2RR) was investigated as a promising technology for the future that could effectively reduce carbon dioxide (CO_2) emissions. Not only can this technique be performed under low-cost ambient conditions but also water and CO_2 which are the two precursors are abundant. Furthermore, if a copper-based catalyst is used, C_{2+} oxygenates, carbohydrates or other carbon compounds can be produced which can be further processed in industry or used as storage for excess renewable electricity from solar and wind power.

The first topic in this work was to study the copper nanocubes while providing controlled mass transport conditions with a gas-tight rotation cell where a rotating cylinder electrode is integrated. This catalyst can produce C_{2+} products with a high activity and lower onset potential. However, there is still no explanation where this effect has its origin. By comparing the experimental results to those obtained by Rüscher [1] on polycrystalline copper, it was found that the enhancement is caused by the nanoporous system. A higher pH value prevails in the pores and the residence time of the intermediates is prolonged, which are perfect conditions for C-C coupling. Furthermore, we were able to gain a better understanding of the catalytic mechanism. Secondly, the design of a catalyst that shows the ability to produce urea during the simultaneous electrochemical reduction of CO_2 and NO_2^- was attempted. Several catalysts based on copper or titanium were investigated but no successful result was achieved and therefore more materials have to be tested in the future. Nevertheless, the copper nanocubes have been shown to also exhibit high selectivity and activity for the electrochemical reduction of NO_2^- to ammonia.

Kurzfassung

In den letzten Jahren hat das Thema Klimawandel immer mehr an Bedeutung gewonnen und der Bedarf an Lösungen zur Verringerung des Verbrauchs fossiler Brennstoffe und der Reduzierung von Treibhausgasen wie Kohlendioxid in der Atmosphäre wird immer dringender. Die Einführung neuer Technologien in der nahen Zukunft ist unumgänglich, da die globale Erwärmung in einem noch nie dagewesenen Tempo voranschreitet. Erneuerbare Energiequellen wie Solarenergie oder Windkraft müssen kostengünstiger werden und die Speicherung des erzeugten Stroms muss verbessert werden.

In dieser Arbeit wurde die elektrochemische Reduktion von Kohlendioxid (CO_2RR) als eine vielversprechende Technologie für die Zukunft untersucht, die Kohlendioxid (CO_2) Emissionen effektiv reduzieren könnte. Diese Technik kann nicht nur unter kostengünstigen Umgebungsbedingungen durchgeführt werden, sondern Wasser und CO_2 , die beiden Ausgangsstoffe, sind auch reichlich vorhanden. Darüber hinaus können bei Verwendung eines kupferbasierten Katalysators C_{2+} -Oxygenate, Kohlenhydrate oder andere Kohlenstoffverbindungen hergestellt werden, die in der Industrie weiterverarbeitet oder als Speicher für überschüssigen erneuerbaren Strom aus Solar- und Windenergie genutzt werden können.

Das erste Thema dieser Arbeit war die Untersuchung der Kupfer-Nanowürfel unter kontrollierten Stofftransportbedingungen mit einer gasdichten Rotationszelle, in der eine rotierende Zylinderelektrode integriert ist. Dieser Katalysator kann C_{2+} -Produkte mit einer hohen Aktivität und einem niedrigeren Onset-Potenzial erzeugen, aber es gibt immer noch keine Erklärung, wo dieser Effekt seinen Ursprung hat. Durch den Vergleich der experimentellen Ergebnisse mit denen von Rüscher [1] auf polykristallinem Kupfer wurde festgestellt, dass die Verstärkung durch das nanoporöse System verursacht wird. In den Poren herrscht ein hoher pH-Wert und die Verweilzeit der Zwischenprodukte ist verlängert, was perfekte Bedingungen für die C-C-Kopplung sind. Außerdem konnten wir ein besseres Verständnis des katalytischen Mechanismus gewinnen.

Zweitens wurde versucht, einen Katalysator zu entwickeln, der die Fähigkeit aufweist, bei der gleichzeitigen elektrochemischen Reduktion von CO_2 und NO_2^- Harnstoff

zu erzeugen. Es wurden mehrere Katalysatoren auf Basis von Kupfer oder Titan untersucht, aber es wurde kein erfolgreiches Ergebnis erzielt, weshalb in Zukunft weitere Materialien getestet werden müssen. Dennoch konnte gezeigt werden, dass die Kupfer-Nanowürfel auch eine hohe Selektivität und Aktivität für die elektrochemische Reduktion von NO_2^- zu Ammoniak aufweisen.

Contents

1	Introduction	1
2	Theoretical Part	4
2.1	CO ₂ RR	4
2.2	Rotating Cylinder Electrode (RCE)	6
2.3	CO ₂ and NO ₂ ⁻ Reduction	7
3	Experimental Part	9
3.1	Experimental Setup	9
3.1.1	CO ₂ RR Gas-tight Rotation Cell	9
3.1.2	CO ₂ and NO ₂ ⁻ Reduction	11
3.2	Electrochemical Methods	12
3.3	Preparation of Catalysts	13
3.3.1	CO ₂ RR	13
3.3.2	CO ₂ and NO ₂ ⁻	13
3.4	Product Detection	15
3.4.1	Nuclear Magnetic Resonance Spectroscopy (NMR)	15
3.4.2	Gas Chromatography (GC)	16
3.4.3	Salicylic Acid Method for Ammonia Detection	16
3.4.4	High Pressure Liquid Chromatography (HPLC) - for Urea Detection	17
4	Mass Transport Effects in CO₂RR	18
4.1	Summary of Results on polycrystalline Copper	18
4.2	Determination of BLT	19
4.3	Preparation of Working Electrode	20
4.4	Influence of Rotation Speed at fixed Potential	21
4.5	Influence of Rotation Speed and Potential Change	23
5	CO₂ & NO₂⁻ Reduction	33
5.1	Copper Group	33

5.2	Titanium Group	36
5.3	Titanium Oxide Group	38
5.4	Comparison of CD and FE towards ammonia	40
6	Conclusion & Outlook	42
6.1	Summary - CO ₂ RR	42
6.2	Outlook - CO ₂ RR	43
6.2.1	New Cell Design	43
6.2.2	Experimental	44
6.3	CO ₂ & NO ₂ ⁻ Reduction - Summary & Outlook	44
	Bibliography	45

List of Figures

2.1	Summary of the efforts to explain the occurring mechanism during the electrochemical CO ₂ RR on copper [15]	5
3.1	Rotation cell [1]	10
3.2	Compression Cell [14]	11
4.1	Results from the ferricyanide reduction experiment where the left graph is showing the change in the mass transport limited regime in dependence of the rotation speed and the right graph offers a comparison of the experimental results with the theoretical expected values	19
4.2	(a) Measured current during the redox-cycling of a polycrystalline copper cylinder in 0.1 M KHCO ₃ and 4 mM KCl for the synthesis of copper nanocubes (b) SEM-Image of the cylinder surface after copper nanocubes synthesis which is clearly revealing the cubic structure. . .	20
4.3	FE and partial CD for major products in dependence of the rotation speed for (a) polycrystalline copper (b) copper nanocubes.	21
4.4	Mass transport scheme for copper nanocubes	22
4.5	Total CD of (a) polycrystalline copper (b) copper nanocubes	23
4.6	Partial CD of hydrogen for (a) polycrystalline copper (b) copper nanocubes	24
4.7	Partial CD of CO for (a) polycrystalline copper (b) copper nanocubes	25
4.8	Partial CD of formate for (a) polycrystalline copper (b) copper nanocubes	26
4.9	Partial CD of ethylene for (a) polycrystalline copper (b) copper nanocubes	27
4.10	Partial CD of methane for (a) polycrystalline copper (b) copper nanocubes	27
4.11	Partial CD of acetaldehyde for (a) polycrystalline copper (b) copper nanocubes and ethanol for (c) polycrystalline copper (d) copper nanocubes	29
4.12	Ratio of aldehydes to alcohols for (a) polycrystalline copper (b) copper nanocubes	30
4.13	Ratio of >2 e ⁻ oxygenates to hydrocarbons for (a) polycrystalline copper (b) copper nanocubes	31

4.14	Ratio of C_{2+} to C_1 products for (a) polycrystalline copper (b) copper nanocubes	32
5.1	(a) Redox-Cycling of polycrystalline copper foil in 0.1 M $KHCO_2$ and 4 mM KCl for synthesis of copper nanocubes (b) polycrystalline copper (b) copper nanocubes	34
5.2	FE and partial CD of products synthesized during the simultaneous electrochemical reduction of CO_2 and NO_2^- for (a) polycrystalline copper (b) copper nanocubes tested at different potentials vs SHE . .	35
5.3	(a) Comparison of gaseous product's CDs for first and second GC injection for polycrystalline copper at -1.14 V vs SHE and copper nanocubes at -1.14 vs SHE (b) Chronoamperometry for polycrystalline copper at -1.14 V vs SHE (black line) and copper nanocubes at -1.14 vs SHE (red line)	36
5.4	(a) Electrodeposition of copper on pre-cleaned titanium foil at -1.5 V vs carbon foil from 140 mL of 0.1 M $CuSO_4$ and 1 M citric acid for 100 seconds (b) copper deposited on titanium	37
5.5	FE and CD of products synthesized during the simultaneous electrochemical reduction of CO_2 and NO_2^- for (a) titanium foil (b) copper deposited on titanium tested at different potentials vs SHE	37
5.6	(a) Anodic growth of titanium oxide in 0.1 M $HClO_4$ at 20 V vs Pt foil (blue line) and in 0.4 M NH_4Cl (pH 1.5) at 18 V vs Pt foil (black line) (b) TiO_2 $HClO_4$ (c) TiO_2 NH_4Cl	39
5.7	FE and CD for products synthesized during the simultaneous electrochemical reduction of CO_2 and NO_2^- for (a) TiO_2 $HClO_4$ (b) TiO_2 NH_4Cl tested at different potentials vs SHE	39
5.8	Comparison of CD (a) and FE (b) of ammonia for all the catalysts tested in the simultaneous electrochemical reduction of CO_2 and NO_2^-	40
6.1	Design of the new gas-tight rotation cell [1]	43
A.1	Calibration curves for H-NMR (a) relative area (b) normalized area .	51
A.2	Calibration curve for ammonia quantification (salicylic acid method) .	51
A.3	(a) Calibration curves for urea (b) chromatogram for 1 mM urea standard	52
A.4	Partial CD of CO normalized with BLT (a) polycrystalline copper (b) copper nanocubes	52
A.5	Partial CD of propionaldehyde for (a) polycrystalline copper (b) copper nanocubes and n-propanol for (c) polycrystalline copper (d) copper nanocubes	53

A.6 Partial CD of remaining products (a) polycrystalline copper (b) copper nanocubes	54
------------------------------------------------------------------------------------------------	----

List of Tables

3.1	Gradient profile for urea detection [32]	17
4.1	Calculated BLT from experimental results	20
4.2	Ethylene to methane ratio for given experimental conditions with the applied potential (V vs SHE) shown in parentheses	28
A.1	Results of calibration for GC	52

List of Abbreviations

Mathematical Symbols

A	Electrode Surface Area [m]
c^0	Bulk Concentration [$\text{mol}\cdot\text{m}^{-3}$]
c_i	Product Concentration [$\text{mol}\cdot\text{m}^{-3}$]
δ	Boundary Layer Thickness [m]
d	Characteristic Dimension [m]
D	Diffusion Coefficient [$\text{m}^2\cdot\text{s}^{-1}$]
F	Faraday Constant [96 485 C $\cdot\text{mol}^{-1}$]
j_i	Partial Current Density [$\text{A}\cdot\text{m}^{-2}$]
j_{lim}	Limiting Current Density [$\text{A}\cdot\text{m}^{-2}$]
j_{tot}	Total Current Density [$\text{A}\cdot\text{m}^{-2}$]
t	Duration of Experiment [s]
U	Peripheral Velocity [$\text{m}\cdot\text{s}^{-1}$]
V	Electrolyte Volume [m^3]
ν	Kinematic Viscosity [$\text{m}^2\cdot\text{s}^{-1}$]
z	Charge Number

Abbreviations

BLT	Boundary Layer Thickness
CD	Current Density
CO ₂ RR	Carbondioxide Reduction Reaction
FE	Faradaic Efficiency
GC	Gas Chromatography
HER	Hydrogen Evolution Reaction
HPLC	High Pressure Liquid Chromatography
NMR	Nuclear Magnetic Resonance
RCE	Rotating Cylinder Electrode
RDE	Rotating Disk Electrode
RHE	Reversible Hydrogen Electrode
SHE	Standard Hydrogen Electrode

Chapter 1

Introduction

Global energy demand is increasing and in the near future there can't be significant decline expected. This is due to the increasing population of our world and industrial growth of developing countries such as India and China. The main energy source is provided by fossil fuels such as coal, oil and gas which puts an incredible burden on our environment since the combustion of such resources is accompanied by the emission of pollutants.

One category of these pollutants is made up by the greenhouse gases where CO₂ is one of the major contributors to global warming. Thereby, humankind has not only increased the concentration of CO₂ inside the atmosphere, by combusting excessive amounts of fossil fuels, but has also interrupted the carbon cycle by deforestation. [2] If drastic changes are not implemented in the next few years, the average surface temperature could rise by 2 - 6 °C by the end of the 21st century as it was predicted by three different studies. [3]

In order to reduce the great dependence on fossil resources, efforts have been made to make the energy market greener by using energy sources as the sun, wind, water and biomass. Even though these techniques are showing lower values for CO₂-emissions they still have some disadvantages when compared to fossil resources. Biomass is not abundant available and therefore huge areas of agricultural landscape has to be exploited to grow more supplies for the power plants. This brings us to the ethnic questions if these resources e.g., land and water should not rather be used for animals or food. Furthermore, the usage of sun, wind and hydro power are accompanied by large investment costs for solar panels, wind wheels etc. which makes the electricity derived from these techniques more expensive. In addition, energy generation with the help of wind and sun requires appropriate meteorological conditions. If there is no sun or wind, then also no electricity can be produced. To ensure a constant energy supply and long-distance transportation with these techniques, the excess electricity

from peak hours has to be converted into a safely and efficiently storable form.

To overcome these problems research in the field of electrochemistry tried to come up with possible solutions where the most promising breakthroughs can be summarized by lithium-ion batteries and hydrogen fuel cells. Even though lithium-ion batteries are showing one of the highest available energy efficiencies on the market the cost of production is very high. [4] Hydrogen provides a very promising future fuel due to its high energy content and low atomic mass and in addition it can be used in power-to-gas applications but still a major part of hydrogen is derived from fossil fuels or biomass. [5]

A more promising technique which is one of the main topics in this work is the electrochemical reduction of CO_2 to which in recent years many research groups have devoted a lot of attention. The idea is to convert CO_2 and water to high energy density compounds which can then be further used in industrial applications or as an energy storage for the excess electricity derived from renewable energy sources as solar and wind power. Thereby, one of the major advantages is that both reactants, CO_2 and water, are abundant. CO_2 can be directly reduced on site from industrial plant emissions, or it can be extracted from the atmosphere. Moreover, this process can be performed under ambient conditions which is also desirable for a lower energy input.

Nevertheless, there are not many industrial applications so far and future work has to be done to further optimize this technique. Especially, when copper is used as a catalyst, which is the only known transition metal that can perform C-C coupling with a high activity, the required high overpotential and the lack of product selectivity are problems that need to be solved. The first goal of this thesis was to investigate a nano porous copper catalyst, called copper nanocubes. This catalyst is revealing a high selectivity, activity and low onset potential for C_{2+} products but the mechanism behind this enhancement is not well understood so far. In this work we are suggesting that the high pH and long retention time of intermediates inside the pores are the main reasons for the high activity towards C-C coupling. This hypothesis is supported by experimental results where the mass transport near the electrode surface was controlled by using a RCE.

The second topic of the work involves the problem of the growing demand of fertilizer through the yearly increasing world population which results in an increasing need of food. Urea is one of the widely used fertilizers due to its high water solubility and nitrogen content. The production of urea is very energy consuming where three plants are included in the process scheme, namely the ammonia plant, utility plant and urea plant. Ammonia is produced through the high energy consuming Haber-

Bosch process and the utility plant is providing electrical energy, water etc. for the urea and ammonia plant. Considering the entire process, one ton of urea requires 12.8 m³ of water and 173.7 kWh of electrical energy. [6]

A more environmentally friendly production method was first discovered by Shibata et al. who was able to electrochemically reduce CO₂ and NO₂⁻ to urea by using zinc as the catalyst. [7]. This method again has the advantage that two of the three precursors, namely CO₂ and water, are abundant. Furthermore, nitrite is a common water pollutant who can have deadly consequence for fish or can cause severe illness for people, especially for newborns. Excessive research was done about the electrochemical denitrification of wastewater in the past years where this process provides another possible future application. [8] In addition, this method can be performed again under ambient conditions and would greatly reduce the burden on the environment compared to the industrial process used so far.

However, the catalytic mechanism is not well understood and only suggestions were made about a CO-like and NH₃-like intermediate which is performing a surface coupling step to give urea as the end product. Therefore, in this work the second goal was to design an active catalyst for urea so that in the next step the intrinsic parameters could be investigated by using the before mentioned gas-tight rotation cell.

Chapter 2

Theoretical Part

2.1 CO₂RR

The electrochemical reduction of CO₂ is a promising future application with the goal to lower CO₂ emissions by converting it into useful chemical compounds in industry. Thereby, excessive electricity from renewable energy sources as solar and wind power can serve as the energy source to drive this thermodynamical endergonic process. Especially, in the last few years this idea received again a lot of attention since CO₂, the most abundant greenhouse gas, is one of the major contributors to global warming.

There are two approaches to develop this process to a feasible economic point. Firstly, the idea is to produce syngas in different composition by reducing CO₂ to CO and water to hydrogen. Therefore, a stable and active catalyst has to be designed which can then be implemented in a gas diffusion electrode for fuel cells. Furthermore, an optimum fuel cell configuration has to be elaborated with which a high net CO₂-consumption can be reached. So far, faradaic efficiencies (FE) over 90 % towards CO at a current density (CD) of 200 mA·cm⁻² by applying a potential of 3 V has been reported. [9] [10] Nevertheless, the net CO₂ consumption for these devices is low since bicarbonate and carbonate ions can diffuse to the counter electrode where they are neutralized or electro-oxidized back to CO₂. [11]

The second approach is focused on converting CO₂ to high energy density compounds as ethanol and propanol. Thereby, it was Hori et al. in the 80s who laid the foundation by reporting that copper is capable of performing C-C coupling when used as a catalyst for the electrochemical reduction of CO₂ [12] [13]. So far, copper remained as the only reported catalyst which can perform C-C coupling with a high activity and a lot of research was done to drive the selectivity towards one product, preferable alcohols. This is of great interest because the very broad product spectrum includes

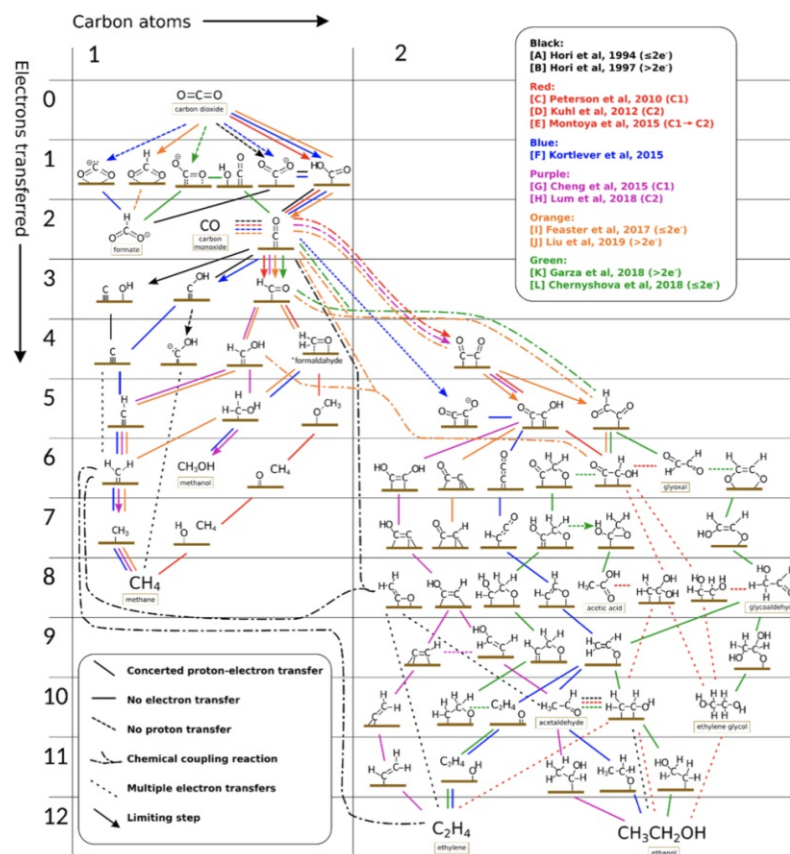


Figure 2.1: Summary of the efforts to explain the occurring mechanism during the electrochemical CO₂RR on copper [15]

16 different molecules catalyzed by 2 to 18 e⁻ transfers and furthermore all of them are revealing a similar onset potential. [14] This makes it necessary to understand the occurring mechanism to systematically optimize the copper surface with the goal to selectively reduce CO₂ to one high energy density compound. Subsequently, this would help to overcome the problem of product separation which plays an important cost factor in future industrial applications. In figure 2.1 a summary of all the efforts done so far to explain the catalytic mechanism is depicted, where the complexity of the CO₂RR can be clearly seen. [15] Hence, there is no agreement on one mechanism and more future experimental investigations combined with theoretical studies have to be done to yield a better understanding.

In previous studies it was tried to enhance the selectivity of copper towards C₂₊ products since those are more valuable from an economic point of view. One way to achieve this higher activity towards C-C coupling was successfully shown by using the so called copper nanocubes as the catalyst. Thereby, cubic structured copper is synthesized by redox cycling polycrystalline copper between -1.15 and 0.9 V vs reversible hydrogen electrode (RHE) in the presence of chloride ions. With this

nanostructured catalyst, especially for ethylene, an enhanced production rate and lower onset potential can be observed, while the activity towards methane decreases. It was speculated that the high degree of (100) surface orientation, revealed by the cubic structured copper, could be the main reason for the high activity towards ethylene. However, this theory doesn't serve as an explanation for the high ethylene to methane ratio. [16] [17] Furthermore, it was shown that non crystal facet favored CuO-oxide derived catalyst are exhibiting very similar results, which further points towards another reason which is causing the high observed ethylene to methane ratio. [18] Therefore, in this study we performed CO₂RR experiments on polycrystalline copper and copper nanocubes while controlling the mass transport by using our state of the art gas-tight RCE setup. Thereby, we want to confirm our hypothesis that the high ethylene to methane ratio is not caused by the favoring of the (100) crystal facets but by the nano porous system of the catalyst. Because the high roughness factor compared to planar electrodes leads to an increased pH near the electrode surface, which was confirmed as one of the enhancement factors towards C-C coupling. [19] Furthermore, the higher residence time of intermediates inside the pores can increase the likelihood of re-absorption and further reduction.

2.2 Rotating Cylinder Electrode (RCE)

In many electrochemical studies it is important to have a defined control of the solution movement since the experimental conditions can be disturbed by unavoidable convection of the electrolyte. Especially, in long-time electrolysis the effect of uncontrolled convection has to be taken into account, since for different electrochemical setups this can lead to a significant change in the obtained results. Thereby, an accurate comparison of experimental data between different literature sources cannot be done successfully.

One solution to overcome this problem is to control the convection of the system in a well-defined way. This can be simply achieved by rotating the electrode and is therefore also a very popular strategy in electrochemistry to study the occurring reaction kinetics of the electrode. By changing the rotation speed the diffusion boundary layer at the electrode surface can be systematically controlled and thereby it allows to investigate electrochemical processes without the random effects of free convection. It can be differentiated between the rotating disk (RDE) and the RCE, whereby the former is mostly used for studies of the reaction kinetics due to its defined laminar flow and well understood mass transport relations.

Nevertheless, in this thesis the RCE was chosen for its higher surface area which is

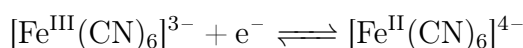
an important factor to detect products from the electrolysis with a higher sensitivity. The limiting CD of a RCE system is described by this empirical equation,

$$j_{lim} = 0.0791 \cdot z \cdot F \cdot c^0 \cdot U^{0.7} \cdot d^{-0.3} \cdot \nu^{-0.344} \cdot D^{0.644} \quad (2.1)$$

which is analogous to the Levich equation for the RDE and it shows that the limiting current has a dependence on the peripheral velocity (U) with a power to 0.7. [20] Furthermore to study the diffusive flux of analytes away and to the electrode surface the knowledge about the boundary layer thickness (BLT) is important which can be derived from the following equation:

$$\delta = \frac{D \cdot c^0 \cdot A \cdot F}{j_{lim}} \quad (2.2)$$

To quantify the limiting CD a facile and reversible reaction with nearly no charge transfer control is needed which is provided by the reduction of ferricyanide ions,



where normally platinum or nickel is used as the catalyst. However, there are some obstacles with these methods as poisoning of the catalysts and gradual decomposition of the ferricyanide ions under the influence of light. [21]

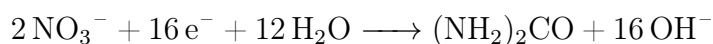
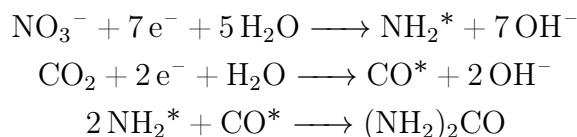
2.3 CO₂ and NO₂⁻ Reduction

Another pollutant, besides CO₂, that should be given much attention is NO_x, since it has severe effects on our health and also shows a negative impact on vegetation. In the past, extensive research has been done to electrochemically reduce nitrate and nitrite species, which can be found as a pollutant in wastewater, to ammonia, which is one the most important industrial precursor for fertilizers e.g., urea. [22]

This prompted the idea to skip one step and directly produce urea by the simultaneous reduction of nitrate/nitrite and CO₂ to urea. The first results were reported by Shibata et al. who tested many different catalysts towards their activity to synthesize urea in a gas diffusion electrode setup. During his studies he investigated most of the transition metals in their metallic state with the result when using nitrite as the nitrogen source Cu and Zn are revealing a FE of 36 % and 55 % at -1 V vs standard hydrogen electrode (SHE) towards urea. [7] [23] [24]. Furthermore, also titanium oxide was reported as a successful catalyst where P25 TiO₂ nanoparticles (Degussa) can reduce nitrate and CO₂ to urea with a FE of 40 % at -0.51 V vs RHE and Cu-doped TiO₂ nanotubes can catalyze urea with a FE of 43.1 % at -0.40 V vs RHE when

using again nitrite as the nitrogen source. [25] [26]

Thereby, the catalytic mechanism of this reaction is not completely understood so far, but it is speculated that a CO-like intermediate and two NH₃-like intermediate can react on the catalyst surface to urea under consumption of 16 e⁻ as shown below when starting from nitrate:



Furthermore, the same experiments were performed by Shibata et al. with CO instead of CO₂ and NH₃ instead of nitrite and no formation of urea could be found. [24] These results further support the before shown reaction scheme where it is proposed that the intermediates which are performing the carbon-nitrogen coupling step must be less reduced species.

In this thesis the goal was to find an active catalyst for the production of urea to subsequently investigate the performance in our RCE-setup to understand how mass transport can affect the product selectivity and gain a better understanding about the occurring reaction mechanism.

Chapter 3

Experimental Part

In this part of the thesis the setup for all the performed experiments will be discussed, including specifics like the used cell, electrolyte etc. Furthermore, the preparation of each tested catalyst will be described, followed by an explanation of the methods which were used to quantify the products of each catalyst.

3.1 Experimental Setup

3.1.1 CO₂RR Gas-tight Rotation Cell

As already mentioned in the introduction, one of the main goals of this thesis is to study the influence of mass transport effects on the product selectivity during the electrochemical reduction of CO₂. To study the mass transport effects not only on the production rate of liquid products but also of gaseous product a gas-tight rotation cell is required. In this thesis a state of the art rotation cell (Fig.3.1) was used which was designed by my fellow students Joonbaek Jang and Martina Rüscher based on the design of Jung et.al [27]. In this case a driver magnet was used which is coupled to a in a Teflon shell encapsulated follower magnet to ensure a gas tight system while rotating the cylindrical working electrode. To achieve a stable electric connection two brush-plungers (Pine Research Instrumentation) where used which are able to compensate any vibration caused by the RCE shaft. A more detailed description of the rotation cell was made by Rüscher. [1]

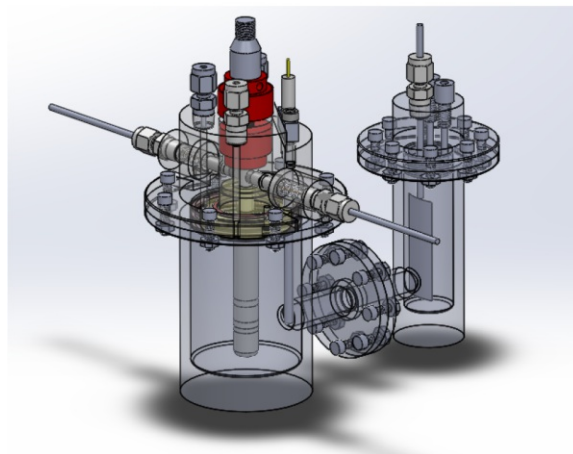


Figure 3.1: Rotation cell [1]

For the electrochemical studies polycrystalline copper and copper nanocubes were tested during the CO_2RR . The experiments on polycrystalline copper have been already performed by my fellow student Rüscher [1] and have been reproduced in this thesis to ensure a good statistical significance of the results.

The setup used for the experiments consisted out of a three-electrode system, where a Ag/AgCl electrode was used as the reference electrode and a platinum foil as the counter electrode. The electrolysis was performed for 78 minutes where the potential was held constant by the potentiostat while correcting for 85 % of the IR-drop. During the whole experiment in both working and counter compartment CO_2 was bubbled, whereby the flow rate at the working side was controlled to 20 sccm by a mass flow controller (MKS Instruments, Model No. GM50A). The electrolyte volume of the working side amounted to 82 mL and for the counter side to 22 mL. Gaseous products were quantified by a gas chromatograph which was linked to the headspace of the working side. The first injection was made after 15 minutes followed by three more injections every 20 minutes. After the experiment an aliquot of the working electrolyte was taken to quantify the liquid products by H-NMR.

To investigate the effect of mass transport a rotation sweep at - 1.41 V vs SHE for polycrystalline copper and at - 1.25 V vs SHE for copper nanocubes was performed. Furthermore, the influence of the applied potential and of two different rotation speeds (100 and 800 rpm) was tested. And last but not least the effect of the buffer concentration was examined by using either 0.1 or 0.2 M potassium bicarbonate as the electrolyte.

3.1.2 CO₂ and NO₂⁻ Reduction

For the simultaneous electrochemical reduction of CO₂ and NO₂⁻ a sandwich type cell (Fig.3.2), designed by Kuhl et.al [14], was used. This kind of cell provides the advantage of a high working electrode area (5.8 cm²) to working electrolyte volume (10 mL) ratio, which is resulting in a very low detection limit for liquid products.

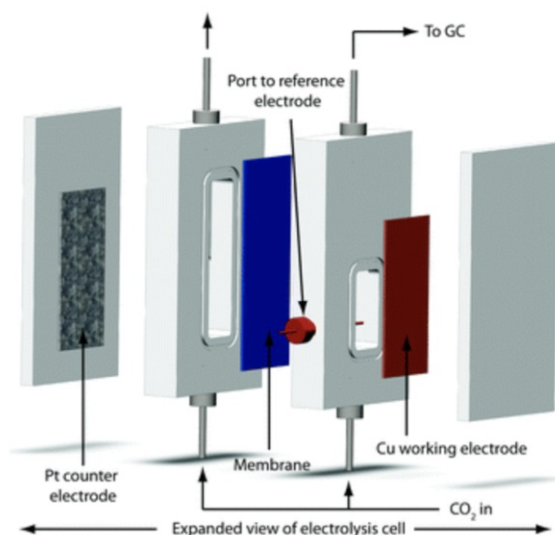


Figure 3.2: Compression Cell [14]

To test the activity of each catalyst for their activity towards urea again a three-electrode setup was used with a Ag/AgCl electrode as the reference electrode and a platinum foil as the counter electrode. The working side as well as the counter side electrolyte volume amounted to 10 mL. The electrolysis was performed for 26.7 min with a constant applied potential whereby 85 % of the IR-drop was compensated. As electrolyte 0.2 M potassium bicarbonate with 0.02 M potassium nitrite, serving as the nitrogen source, was used. Both the working side and the counter side was bubbled with CO₂ and again the flow rate in the working compartment was controlled to 20 sccm.

The headspace of the working side was connected to the gas chromatograph to quantify the gaseous products. The first injection was made after 5 minutes followed by a second one after 20 minutes. After the experiment the working electrolyte was tested for liquid products with H-NMR, for ammonia with the salicylic acid method and for urea with HPLC.

3.2 Electrochemical Methods

For all the electrochemical methods explained in the following section a potentiostat (PGSTAT302N) from Autolab was used. The data evaluation program NOVA was used for analyzing all the obtained data.

Chronoamperometry

Chronoamperometry was used for all the performed electrolysis during this thesis. Thereby, a constant potential was applied and the current resulting from the faradaic process at the electrode surface was recorded over the whole time.

Cyclic Voltammetry (CV)

To study the electrochemical activity of each tested catalyst a linear cyclic voltammogram was measured before performing the actual experiment. Thereby, the potential was scanned with a scan speed of $50 \text{ mV}\cdot\text{s}^{-1}$ and the resulting current was recorded. This can provide a first insight on the electrochemical processes happening at different potentials and in addition the electrode can be conditioned for the following electrolysis e.g., reduction of copper oxide.

Electrochemical Impedance Spectroscopy (EIS)

The electrochemical impedance spectroscopy is a powerful method in electrochemistry and can be used to determine the impedance of the electrochemical system by changing the frequency of the alternating current. In this thesis EIS was used to determine the resistance of the used electrolyte prior to the electrolysis to correct for 85 % of the IR-drop.

Rotation System

For controlling the mass transport during the CO_2RR the rotation speed of the working electrode has to be controlled. To achieve a stable rotation speed a modulated speed rotator from Pine Research was used. This setup consisted out of the motor assembly and the control unit where the rotation speed was varied manually by turning the black knob in the front.

3.3 Preparation of Catalysts

3.3.1 CO₂RR

in this section the preparation of the polycrystalline copper and copper nanocubes, used as catalysts for the CO₂RR experiments, is going to be described.

Polycrystalline Copper

Copper cylinders with a surface area of 3 cm² were purchased from Pine Research and prepared as followed before used for the electrochemical studies.

To get rid of surface contaminations the cylinder was first mechanical polished with a 600 grit sandpaper and after a rinsing step with deionized water again polished with a 0.05 μm Alumina slurry (Allied High Tech Products Inc.) on a micro-cloth. Subsequently, the copper cylinder was ultrasonicated two times for 10 minutes in deionized water.

After the mechanical treatment an electrochemical polishing step was performed to achieve a smoother surface. Therefore, the electrode was immersed in 85 % phosphoric acid and surrounded by a hollow copper cylinder as counter electrode. In the next step a potential of 1.6 V was applied for 300 seconds.

Copper Nanocubes

For the preparation of the copper nanocubes the copper cylinder was treated in the first step as already described for the polycrystalline copper. Subsequently, the freshly prepared electrode was immersed in 140 mL of 0.1 M potassium bicarbonate containing 4 mM potassium chloride. A three-electrode setup was used with a Ag/AgCl electrode as reference electrode and a carbon foil as counter electrode. The electrode was cycled three times with a scan speed of 5 mV·s⁻¹ from 1.5 to 0.5 V vs SHE and the process was stopped at a potential of 1.0 V vs SHE. Through this process a nanostructured surface with a higher surface roughness compared to the polycrystalline copper can be achieved. [28]

3.3.2 CO₂ and NO₂⁻

In the following paragraphs the preparation of the catalysts tested for their activity towards the production of urea will be described.

Polycrystalline Copper and Copper Nanocubes

The preparation of polycrystalline copper and copper nanocubes is very similar to the described preparation in chapter 3.3.1. The main difference is that in this case copper was used as a foil and not in the form of a cylinder. Furthermore, the mechanical polishing step with the 0.05 μm alumina slurry was not performed. All the other steps, including the electrochemical polishing and the synthesis of the copper cubes were performed in the exact same manner.

Titanium

For testing titanium as a catalyst, a titanium foil was purchased from Fisher Scientific and used as it was delivered. Only two cleaning steps were performed which included ultrasonication in deionized water and acetone for 10 minutes to get rid of surface contaminations.

Copper-Titanium

To test the activity of copper and titanium together as a catalyst towards urea copper was electrochemical deposited on the titanium foil. Thereby, the pretreatment of the titanium foil was performed in the same way as described in the previous paragraph. For the deposition process the foil was immersed in 140 mL of 0.1 M CuSO_4 and 1 M citric acid. In the next step a cathodic potential of 1.5 V was applied for 100 seconds where a carbon foil was used as the counter electrolyte.

Titanium Oxide

As the last catalyst, titanium oxide was tested for its activity towards the production of urea. Thereby, the goal was to achieve the growth of titanium oxide nanotubes, since in a earlier work the formation of urea was reported by using this kind of morphology. [29] Furthermore, a high surface area catalyst would be beneficial because by that more active sites are available, providing a higher stability and durability during the electrolysis.

Based on the results of former studies on the growth of titanium oxide nanotubes, where instead of a fluoride containing a chloride containing electrolyte was used, two different methods were investigated. [30] [31]. The general setup consisted of a glass cell containing 140 mL of the tested electrolyte. For this synthesis a high overpotential has to be applied. Therefore a power supply from Chroma (Model

62012P-40-120) was connected with crocodile clips to the electrodes and a platinum foil was used as the counter electrode. The titanium foil, which was connected as the working electrode to the power supply, was additionally, to the previous explained pretreatment steps, rinsed with concentrated nitric acid.

The tested electrolytes were 0.1 M perchloric acid and 0.4 M ammonium chloride where for the latter one the pH was adjusted to 1.5 by adding a small amount of concentrated hydrochloric acid. In the first case a potential of 20 V and in the second case a potential of 18 V was applied for 1 minute.

After the growth the crystal structure of the titanium oxide is amorphous, therefore an annealing step was performed under ambient atmosphere with a muffle oven (Vulcan 3-550) from Ney. For the heat treatment the temperature was first raised to 200 °C with a ramp rate of 20 °C·min⁻¹ and then heated to 400 °C within 10 minutes which was then also held constant for two and a half hours.

3.4 Product Detection

All of the detectable products were quantified with the following explained methods. With the concentration determined, the FE was calculated using equation:

$$FE = \frac{z \cdot c_i \cdot V \cdot F}{A \cdot t \cdot j_{tot}} \cdot 100 \quad (3.1)$$

Furthermore, the partial CD of each product was calculated by

$$j_i = \frac{FE \cdot j_{tot}}{100}. \quad (3.2)$$

3.4.1 Nuclear Magnetic Resonance Spectroscopy (NMR)

For the determination of liquid products inside the working and counter electrolyte proton nuclear magnetic resonance spectroscopy was applied. In this work for all the measurement a DRX500 spectrometer (Bruker Biospin GmbH) was used. Since all the experiment were performed in an aqueous electrolyte solvent suppression was used to decrease the size of the water peak for better visibility of the peaks arising from the products.

For quantification 35 μL containing 1 mM phenol and 1 mM DMSO in D₂O was added to 700 μL of the electrolyte as an internal standard. A calibration curve for each product was made by comparing the area of the peak of interest to the area of the phenol peak for products at the left side and to the area of DMSO for products at the right side of the water peak (Fig.A.1). For very volatile compounds as acetaldehyde

and propionaldehyde it is hard to achieve a reliable calibrations curve. In this case, an average of all the normalized slopes of the other products was used for a more accurate quantification.

3.4.2 Gas Chromatography (GC)

Gaseous products from the electrolysis were detected on-line by a gas chromatograph coupled to the outlet of the working side of the cell. In this setup, a gas chromatograph from SRI Instruments (Model Number 8610 C) was used which was equipped with three columns. The first column was a 0.5 meter Hayesep-D precolumn followed by a 1 meter MoleSieve 5 Å column for separation of hydrogen, carbon monoxide and methane, and a 2 meter Hayesep-D column for separation of ethylene and ethane. After passing the columns the gas stream was first analyzed for hydrogen by a thermal conductivity detector and then for hydrocarbons by a flame ionization detector equipped with a methanizer. As carrier gas nitrogen was used.

For quantification a one point calibration was made by using a nitrogen calibration standard containing ~ 1000 pm of each of the above mentioned gaseous products (Tab.A.1).

3.4.3 Salicylic Acid Method for Ammonia Detection

To quantify the amount of nitrite reduced to ammonia during the electrolysis the salicylic acid method was used. [26] Thereby, ammonia is reacting with salicylic acid to an intensely colored compound which can be selectively quantified by measuring the absorption at 660 nm. Since this method is only working for ammonia concentrations up to $1.2 \text{ mg}\cdot\text{L}^{-1}$ the first step was to dilute the working electrolyte into the working area of this method with deionized water.

After that, to 8 mL of the diluted working electrolyte 1 mL of reagent A (5 g salicylic acid, 5 g sodium tartrate tetrahydrate and 8 g sodium hydroxide solved in 100 mL deionized water), 100 μL of reagent B (0.1 g sodium nitroferricyanide dehydrate solved in 10 mL deionized water) and 100 μL of 10 - 15 % sodium hypochlorite solution were added and in the end filled up with deionized water to achieve a final volume of 10 mL.

After 60 minutes of reaction time the absorption of the solution was measured with a DU 800 spectrometer (Beckman Coulter). Thereby, a blank sample was used to auto zero the system. The calibration curve which was used to quantify the ammonia content is depicted in figure A.2

3.4.4 High Pressure Liquid Chromatography (HPLC) - for Urea Detection

For the quantification of urea, a derivatization with xanthydroxol to N-9H-xanthen-9-ylurea was performed. After that, the reaction mixture was injected into a reversed-phase - HPLC where after the column the derivatization product was detected with a UV-Vis detector at 210 nm.

For the derivatization of urea the working electrolyte was diluted with 20 v% Ethanol to secure a good solubility of the N-9H-xanthen-9-ylurea. In the next step to 500 μL electrolyte 100 μL of 0.02 M xanythydroxol in n-propanol and 75 μL of 1.5 M hydrochloric acid was added. After a reaction time of 6 minutes in the dark 50 μL of the solution was injected into the HPLC-system (Agilent 1200).

The separation was performed with a Zorbax Eclipse XDB C-18 column (5 μm , 4.6 x 150 mm) from Agilent where a gradient elution with acetonitrile (Solvent A) and 20 mM sodium acetate (Solvent B) at 35 °C was applied. The same gradient profile as described by Clark et.al [32] was used and is summarized in table 3.1. At the end of the column the derivatized product was detected at an absorption wavelength of 210 nm with a slit with of 16 nm.

Table 3.1: Gradient profile for urea detection [32]

Time (min)	Solvent (%B)	Flow rate ($\mu\text{L}\cdot\text{min}^{-1}$)
0	20	0.45
0.06	20	0.45
12.6	50	0.45
13.6	100	0.45
20.6	100	0.8
22.6	20	0.45
23.6	20	0.45

To secure a low impact of possible matrix effect to every prepared standard 2 mM ammonium chloride, 200 mM potassium bicarbonate and 10 mM potassium nitrite was added, since the possible effects of these anions and cations on the occurring derivatization reaction haven't been studied. The obtained calibration curve and a chromatogram, where it can be seen that the N-9H-xanthen-9-ylurea is eluted at a retention time of 15.5 min, are shown in figure A.3

Chapter 4

Mass Transport Effects in CO₂RR

4.1 Summary of Results on polycrystalline Copper

In this section a short summary will be given about how mass transport is affecting the product selectivity on polycrystalline copper in the CO₂RR. A more detailed description can be found in the thesis of my fellow student Rüscher [1]

- Higher rotation speed led to an increase in the flux of intermediates, especially for carbon monoxide, away from the electrode surface and was thereby decreasing the partial CD of further reduced products.
- Higher potassium bicarbonate concentration leads to a lower pH near the electrode surface. Firstly, this resulted in a lower amount of C₂₊ products as has been already reported in the literature. [19] Secondly, a shift in the product selectivity towards hydrogen was observed since bicarbonate can function as a proton donor and lower pH is favoring the Hydrogen Evolution Reaction (HER).
- Higher potential led to a lower oxygenate to hydrocarbons ratio whereas lower rotation speed and higher bicarbonate concentration were affecting the product distribution in the same way.
- Furthermore, the kinetic model which was used to determine the flux of CO₂ to and of the products away from the surface gave an interesting insight on the concentration of species near the electrode surface. Combined with the extracted knowledge of the pH gradient and of the mass transport influence on the product selectivity this model could exhibit a better understanding on the reaction pathway.

4.2 Determination of BLT

To quantify the effect of the rotation speed on mass transport the BLT is a valuable parameter. Therefore, the limiting CD was determined at different rotation speeds for the reduction of ferricyanide from which subsequently the BLT was calculated with equation 2.2.

This experiment was performed in a glass cell with a similar geometry as the working side of the used cell to prevent contamination with iron since this could lead to falsified results during the CO₂RR experiments (enhancement of HER). As supporting electrolyte 0.1 M KClO₄ with 10 mM ferricyanide and as the working electrode the same polycrystalline copper cylinder was used as in all the CO₂RR experiments.

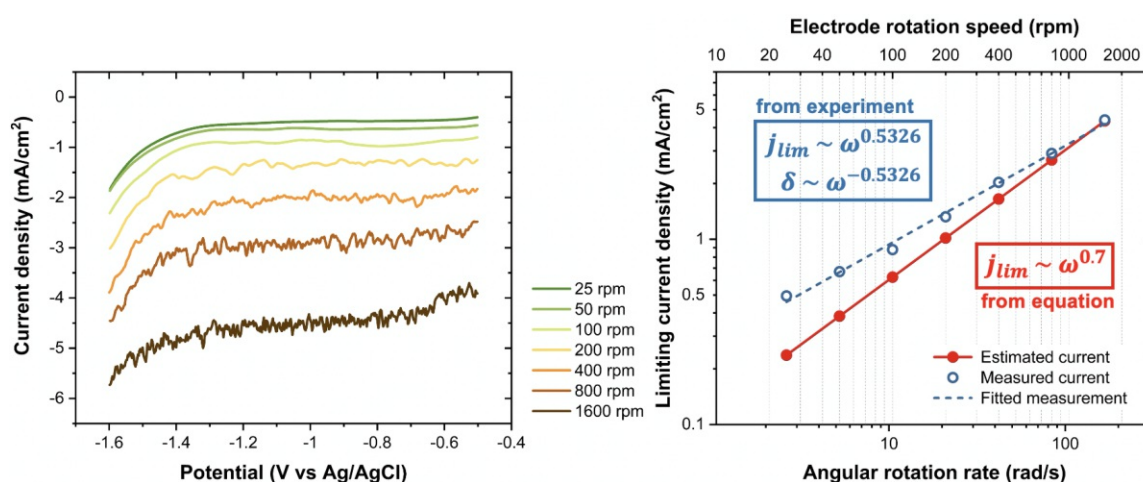


Figure 4.1: Results from the ferricyanide reduction experiment where the left graph is showing the change in the mass transport limited regime in dependence of the rotation speed and the right graph offers a comparison of the experimental results with the theoretical expected values

The results are shown in figure 4.1 where the left graph clearly reveals that with higher rotation speed an increase in the CD can be observed due to a decrease of the BLT. By plotting the averaged CD of the mass transport limited regime against the angular rotation speed a dependence to the power of 0.53 can be derived from the fit. This deviation to the theoretical expected dependence to the power of 0.7 (equ.2.1) could come from several reasons where different hydrodynamic effects of the glass could serve as the most obvious explanation. For sure, future studies have to be done to find the cause of this deviation.

Nevertheless, the resulting BLT from the experimental results were used for all the upcoming investigations in the CO₂RR experiments and are summarized in table 4.1.

Table 4.1: Calculated BLT from experimental results

Rotation Speed [rpm]	100	200	400	600	800
BLT [μm]	79.8	53.0	34.6	28.1	24.1

4.3 Preparation of Working Electrode

The nanostructured copper surface was prepared as already mentioned in chapter 3.3.1 by cycling the cylinder electrode between -1.5 V and 0.5 V vs SHE for three times in the presence of chloride ions.

The current which was measured during the synthesis is shown in figure 4.2 where also a SEM image after the synthesis is depicted which is clearly exhibiting the successful preparation of the cubic morphology. An increase in the current with each cycle can be observed which is probably due to an increase in the surface area. Furthermore, the peak which can be seen at approximately -0.75 V vs SHE can be assigned to the reduction of Cu₂O back to metallic Cu.

In a previous study it was speculated that the formation of the cubic structure is associated with the formation of CuCl₂ on the surface at less oxidative potentials. [16] This was refuted by insitu-XAFS investigation of Eilert et al. where he was not able to detect any CuCl₂ species during the synthesis. Hence, he suggested that the presence of Cl⁻ ions could lead to a different oxidation mechanism where Cu atoms are extracted from the lattice followed by dissolution and precipitation. [18]

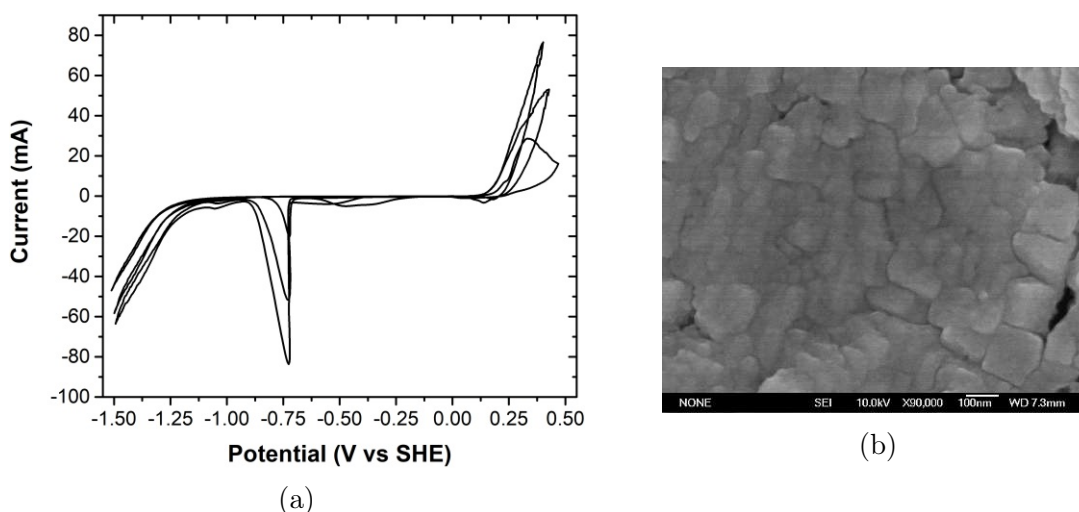


Figure 4.2: (a) Measured current during the redox-cycling of a polycrystalline copper cylinder in 0.1 M KHCO₃ and 4 mM KCl for the synthesis of copper nanocubes (b) SEM-Image of the cylinder surface after copper nanocubes synthesis which is clearly revealing the cubic structure.

4.4 Influence of Rotation Speed at fixed Potential

First of all, the influence of the rotation speed on the product selectivity was investigated at a fixed potential for the copper nanocubes. Therefore, experiments were performed at -1.25 V vs SHE while changing the rotation speed from 100 to 800 rpm. Furthermore, the effect of the buffer concentration was also taken into account by using either 0.1 or 0.2 M KHCO_3 as the electrolyte. In the former studies of Rüscher [1] on polycrystalline copper a more negative potential was applied (-1.41 V vs SHE) which was not doable in this study since the copper nanocubes are revealing

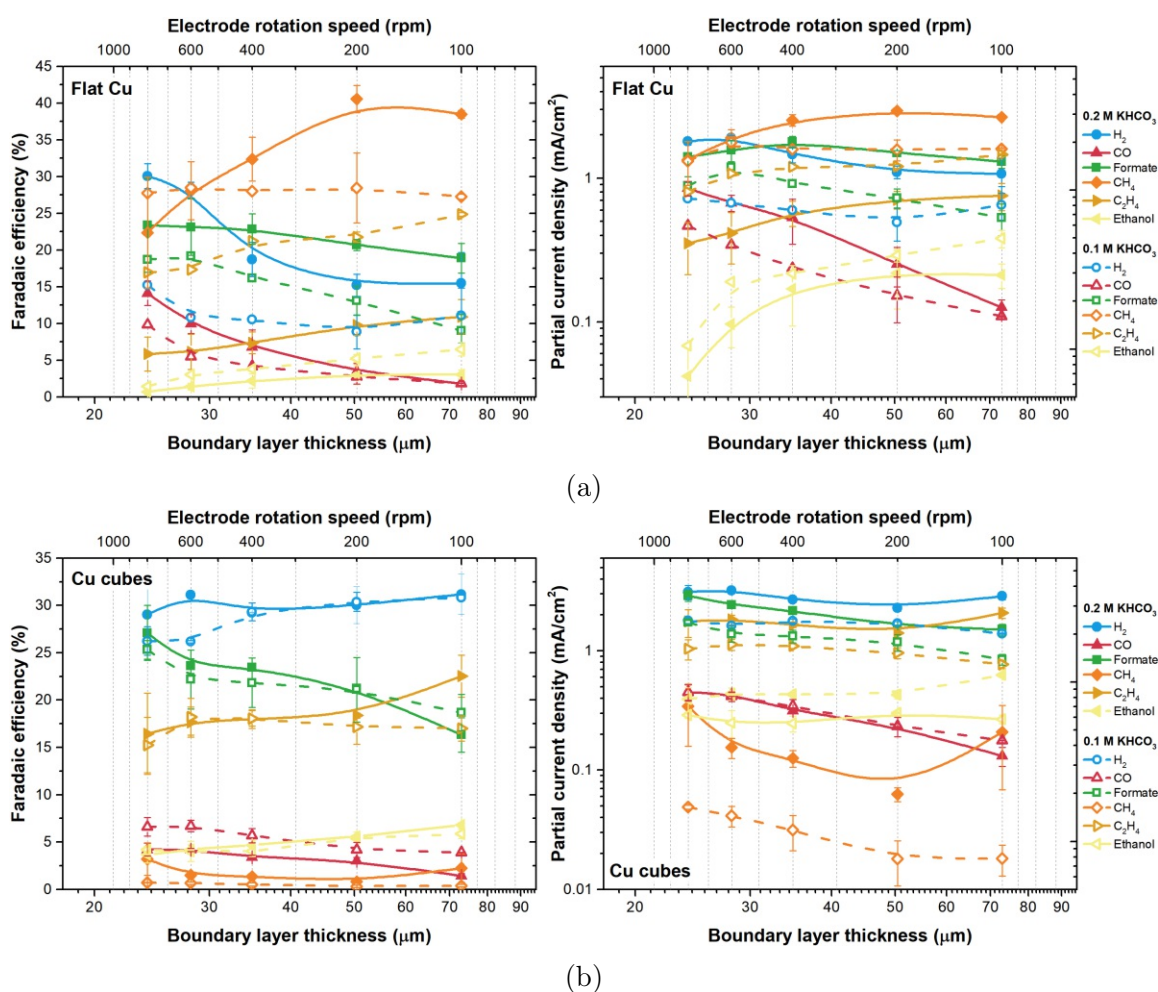


Figure 4.3: FE and partial CD for major products in dependence of the rotation speed for (a) polycrystalline copper (b) copper nanocubes.

a higher total CD. As a consequence, the maximum applicable voltage of the used potentiostat (40 V) was already reached at a less negative potential. This limitation is resulting from the high resistance between the working and counter electrode caused by the large distance and small cross section of the ion bridge. Nevertheless, the experimental results for copper nanocubes from this study were compared to the

data gathered by Rüscher [1] on polycrystalline copper since the copper nanocubes are already revealing the same product spectrum at this lower potential. The FE and CD for the major products of both catalysts are shown in figure 4.3 where each data point is the average of one to three experiments. Furthermore, at this point it can be mentioned that the results from Rüscher [1] were successfully reproduced.

For polycrystalline copper the already mentioned trend can be observed where with higher rotation speed the product selectivity is changing towards CO since the higher rotation speed is resulting in an increased flux of this intermediate away from the electrode surface. As a consequence, the retention time and likelihood of re-absorption is decreasing and therefore it is accompanied by a decrease of the CD towards further reduced species as methane, ethanol and ethylene. Furthermore, no significant influence on the formation of hydrogen and formate could be observed.

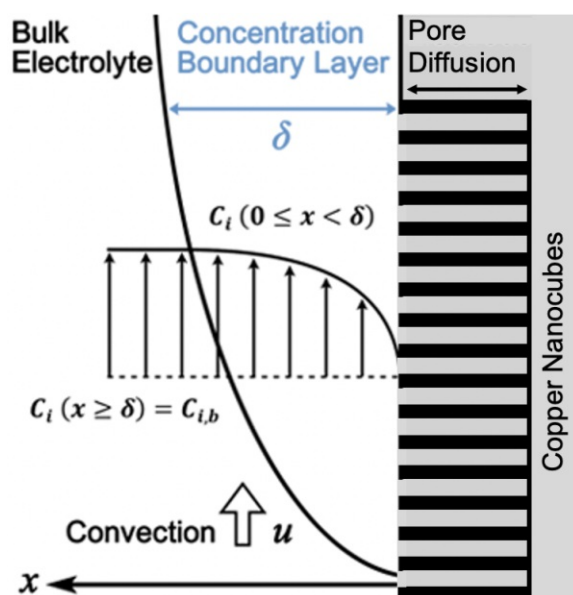


Figure 4.4: Mass transport scheme for copper nanocubes

The copper nanocubes are revealing the same trend for CO where it can be again seen that higher rotation speed is favoring the partial CD of this 2 e⁻ product. Furthermore, hydrogen is again not significantly influenced by the changing BLT and formate is revealing a slight increase with higher rotation speed. However, the more striking observation is that, in contrary to the polycrystalline copper, changes in the rotation speed have no significant impact on the partial CD of further reduced products as ethanol or ethylene and even an increase in the production rate of methane can be quantified. One possible explanation can be provided by the additional pore diffusion resulting from the nano porous structure of the copper nanocubes (Fig.4.4). By changing the rotation speed and thereby the thickness of the boundary layer

only the flux of the species away and to the electrode surface is influenced but not the flux inside the pores. Hence, only the retention time of intermediates at the outermost surface of the catalyst is decreased while inside the porous system, which is making up the biggest part of the active surface area, is not influenced by the rotation speed. These experimental observations further support that the enhancement of C-C coupling for copper nanocubes is not exhibiting from the (100)-crystal facet favoring but rather from the nanostructured porous system which is increasing the likelihood of intermediates readsorbing and being further reduced to C_{2+} products.

Moreover, it can be seen that the $KHCO_3$ concentration has a significant impact on the CD of the products and is going to be discussed in the following sections.

4.5 Influence of Rotation Speed and Potential Change

Next the potential dependence will be described for two different rotation speeds (100 & 800 rpm) and for 0.1 and 0.2 M $KHCO_3$ as the electrolyte. For polycrystalline copper it has been already described by Rüscher [1] that the rotation speed has no significant effect on the total CD and that higher bicarbonate concentration leads to an increase mainly induced by a higher production rate of hydrogen. In general, for the copper nanocubes a higher current can be measured due to the higher surface area of the nano porous system. Furthermore, the same trend could be observed for the bicarbonate concentration but now also higher rotation speed leads to an increase in the total CD (Fig.4.5).

For an better examination of the potential dependence with different BLTs and $KHCO_3$ concentrations the major products will be described individually in the fol-

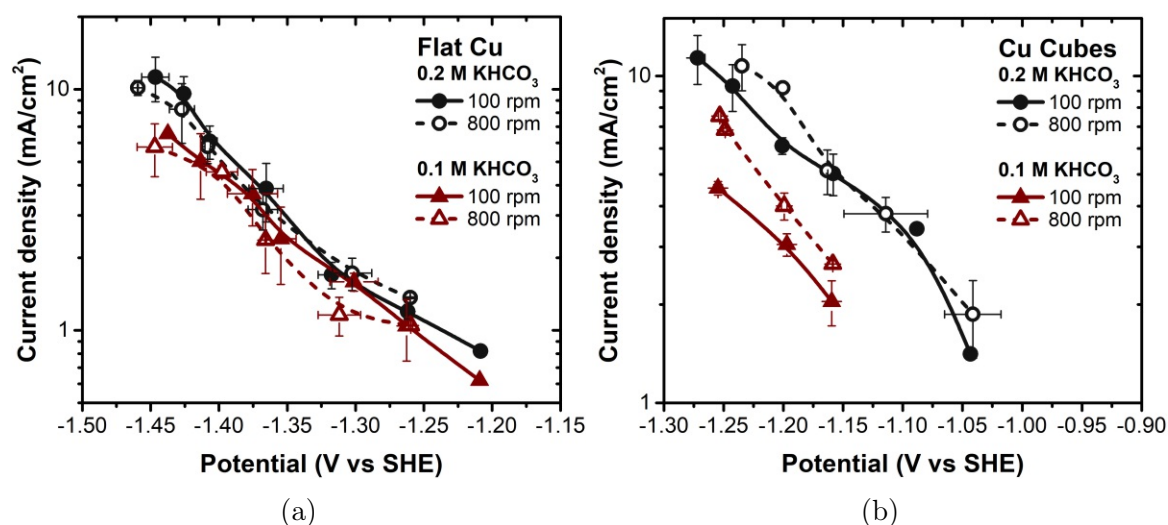


Figure 4.5: Total CD of (a) polycrystalline copper (b) copper nanocubes

lowing sections.

Hydrogen

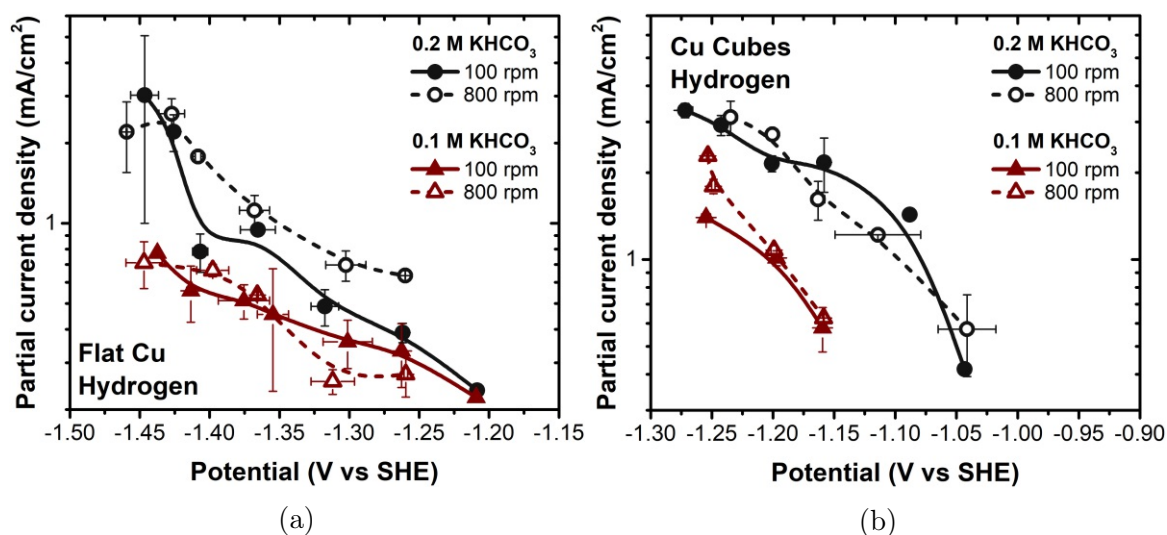


Figure 4.6: Partial CD of hydrogen for (a) polycrystalline copper (b) copper nanocubes

It is well known that the formation of hydrogen is showing a high pH dependence, where a lower pH value means a higher number of protons which subsequently leads to an increase in the partial CD of hydrogen. In the investigated system either water or KHCO₃ molecules can serve as a proton donor to drive the HER.

Comparing the HER for polycrystalline copper and copper nanocubes the same trend can be observed during the CO₂RR (Fig.4.6). A higher bicarbonate concentration leads to an enhancement of the HER by serving as a proton donor and lowering the pH near the surface by consuming the hydroxy ions which are a byproduct of the CO₂RR. From the mathematical model of Rüscher [1], which serves as a good description for the diffusive flux of species, it can be derived that the rotation speed has an impact on the pH near the electrode surface. Nevertheless, for both catalysts no significant dependence of the rotation speed on the partial CD of hydrogen could be observed.

Carbon monoxide

Carbon monoxide is one of the most important intermediates in the CO₂RR on copper where Hori et al. was able to show that most of the products including, methane,

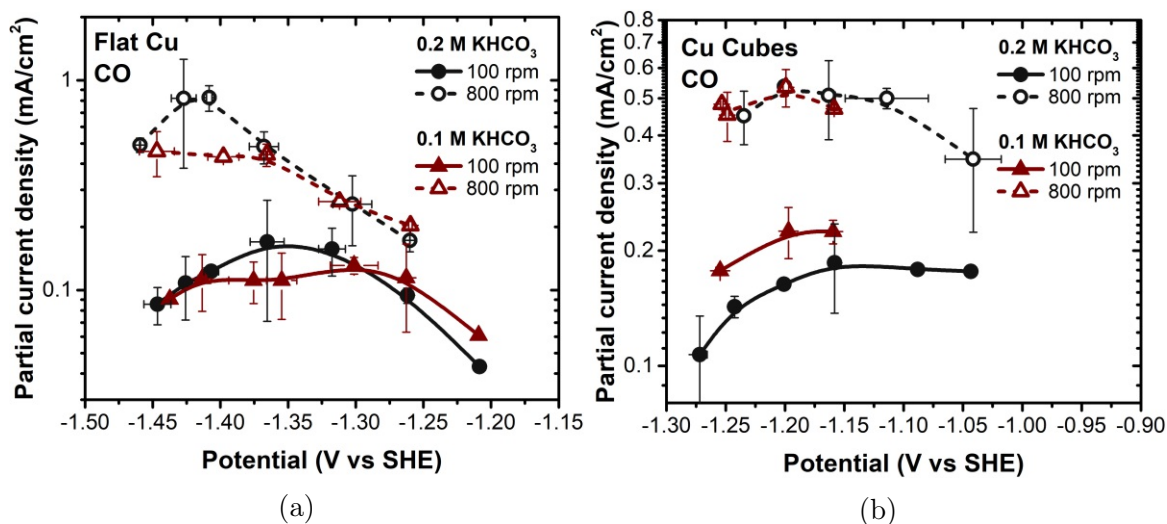


Figure 4.7: Partial CD of CO for (a) polycrystalline copper (b) copper nanocubes

ethylene and C_{2+} aldehydes and alcohols are sharing CO as an intermediate. [33] Rüscher [1] was able to confirm these results by showing that a higher rotation speed increases the flux of CO away from the surface which is accompanied by a decrease of the production rate of the before mentioned products.

For CO again the same trend for polycrystalline copper and copper nanocubes can be observed where the partial CD is significantly impacted by the rotation speed but not by the $KHCO_3$ concentration (Fig.4.7). This dependence on the diffusive flux away from the surface is better illustrated in figure A.4 where the CD is normalized by the BLT using equation 2.2. Furthermore, it can be seen that in the plateau region the production rate of CO is increased sevenfold for the flat copper while for the copper nanocubes it is only tripled. This further suggests that carbon monoxide is preferentially desorbed from the outermost electrode surface area while it is further reduced inside the pores where it cannot escape.

Formate

Formate is the second $2 e^-$ product of the CO_2RR which is yielded with a high selectivity. Former studies suggests that it is a terminal product which is synthesized by the reduction of CO_2 over a formyl intermediate (Fig.2.1). [34] [35]

For polycrystalline copper Rüscher [1] could already observe that in contrary to other further reduced products the partial CD of formate is increasing with higher rotation speed when the experiments were performed in 0.1 M $KHCO_3$ but is not influenced by the changing BLT in 0.2 M $KHCO_3$ (Fig.4.8). In combination with the results gathered for the copper nanocubes where higher rotation speed and higher buffer

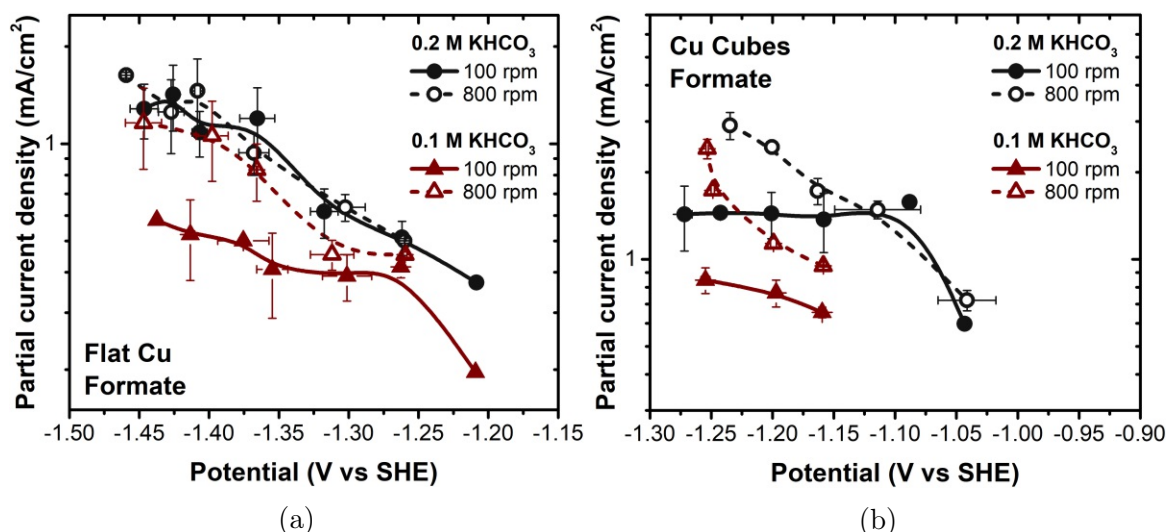


Figure 4.8: Partial CD of formate for (a) polycrystalline copper (b) copper nanocubes

concentration is exhibiting an enhancement for the partial CD of formate it can be concluded that the formation of this product should be influenced by the convolution of two factors. Firstly, a higher rotation speed is increasing the concentration of CO_2 near the electrode surface and could thereby increase the partial CD. Secondly, a higher KHCO_3 could enhance the formation of formate by either serving as a proton donor or by suppressing the other pathway towards CO .

Ethylene

Driving the selectivity of the CO_2RR towards ethylene is very desirable since it is a popular chemical compound in the industry. Therefore, nanostructured copper catalysts e.g., copper nanocubes became famous by increasing the selectivity of ethylene over methane and revealing a lower onset potential for this C_{2+} product. [16] For polycrystalline copper Rüscher [1] could observe that higher rotation speed and KHCO_3 concentration leads to a suppression in the formation of ethylene. The influence of the rotation speed nearly disappears for the copper nanocubes since this product could be preferentially synthesized inside the pores as already discussed in chapter 4.4. In contrary, to the polycrystalline copper 0.2 M KHCO_3 is leading to a higher partial CD of ethylene which is also not in agreement with studies reported in the literature where it was shown that higher pH is leading to an enhancement when performing CORR on copper cubes. [17] This could be explained by the following buffer reactions which are occurring when KHCO_3 is used as the electrolyte:

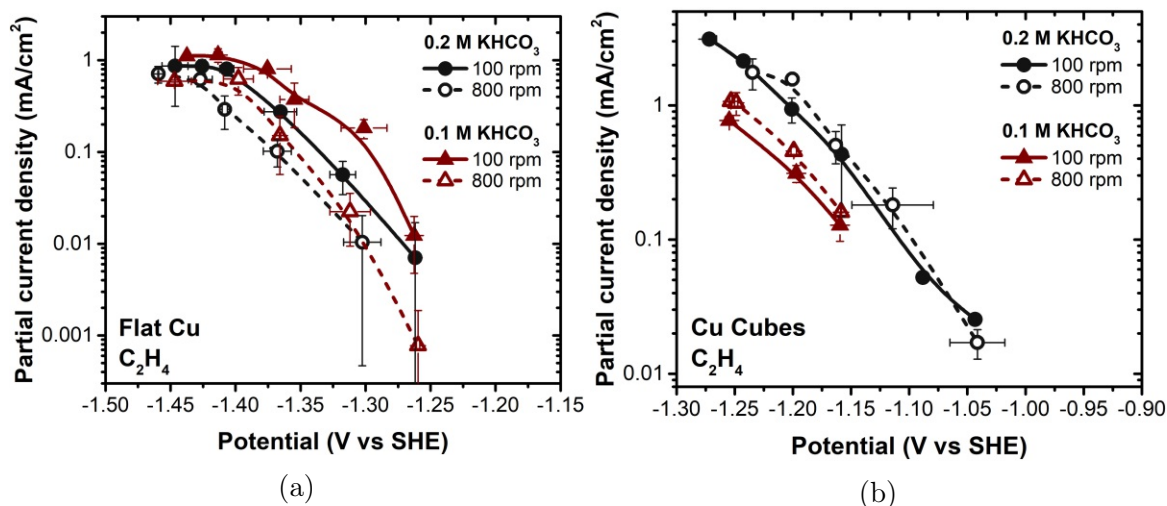
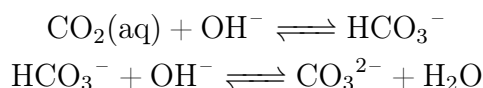


Figure 4.9: Partial CD of ethylene for (a) polycrystalline copper (b) copper nanocubes



Due to the high pH inside the pores of the copper nanocubes CO₂ could be predominantly consumed by the hydroxyl ions and not by the electrochemical process. Subsequently, less coverage of intermediates can be expected which could lead to the observed suppression in C-C coupling.

Methane

Next methane is going to be discussed which is one of the major products for poly-

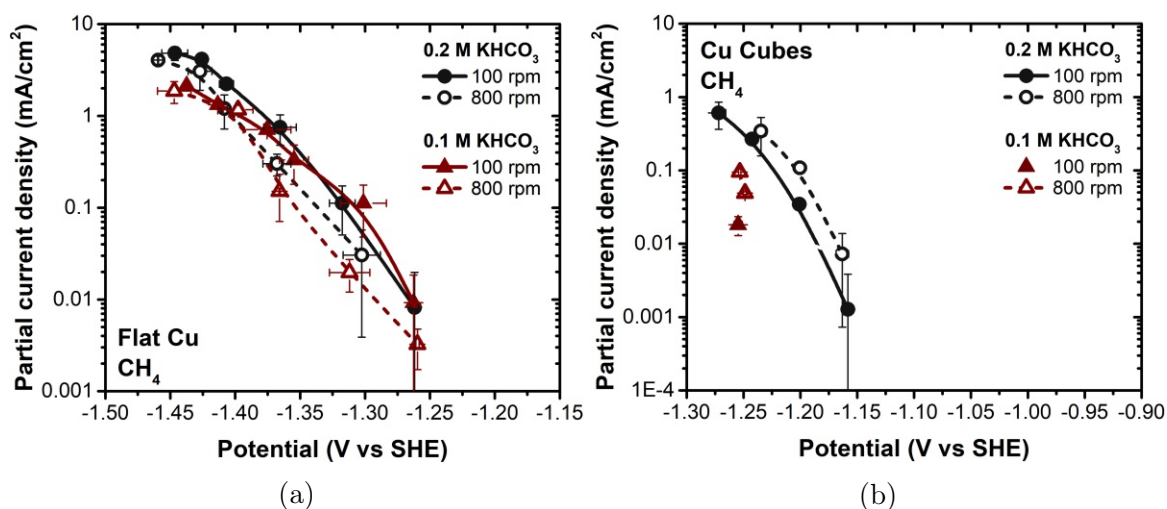


Figure 4.10: Partial CD of methane for (a) polycrystalline copper (b) copper nanocubes

crystalline copper but is suppressed when using copper nanocubes as a catalyst for the CO₂RR. For both catalysts higher bicarbonate concentration is favoring the formation of methane since it can act as a proton donor for this highly hydrogenated product. Furthermore, an inverse trend can be noted for the rotation speed where shorter BLT is giving an increase in the partial CD for copper nanocubes but a decrease can be observed for polycrystalline copper.

The more striking result which should be emphasized is the high formation of ethylene over methane for the copper nanocubes, where methane couldn't even be detected at low overpotential when using 0.1 M KHCO₃ as the electrolyte. In table 4.2 the ethylene to methane ratio for the lowest overpotential at which both products were detectable are summarized. It can be seen that higher pH at the electrode surface and a lower rotation speed is desirable to yield a higher selectivity towards ethylene for both catalysts.

Table 4.2: Ethylene to methane ratio for given experimental conditions with the applied potential (V vs SHE) shown in parentheses

	Poly. Cu		Cu Nanocubes	
	100 rpm	800 rpm	100 rpm	800 rpm
0.1 M KHCO ₃	1.33 (-1.26 V)	0.239 (-1.26 V)	42.7 (-1.25 V)	11.3 (-1.25 V)
0.2 M KHCO ₃	0.506 (-1.26 V)	0.341 (-1.30 V)	5.13 (-1.27 V)	5.14 (-1.23 V)

Aldehydes & Alcohols

Next the partial CD of aldehydes and alcohols will be discussed with a special focus on acetaldehyde and ethanol. These two oxygenates are described together since it was shown that aldehydes are possible intermediates on the CO₂RR pathway to alcohols. Thereby, Hori et al. was able to electrochemically reduce formaldehyde, acetaldehyde and proprionaldehyde to methanol, ethanol and n-propanol on copper. [36]

For polycrystalline copper the same trend for both products as already mentioned before for ethylene could be observed by Rüscher [1] where higher rotation speed and KHCO₃ concentration is leading to a decrease in the partial CD. In contrary, an increase in the activity towards acetaldehyde can be observed for the copper nanocubes with higher rotation speed while the buffer concentration has no significant influence. The experimental results for ethanol are exhibiting the same dependence on rotation speed and buffer concentration as already explained for ethylene (Fig.4.11). The increase in the formation of acetaldehyde for copper nanocubes is providing further evidence that it is one of the early C-C coupling intermediates which are able to leave the copper surface since CO is showing the same behavior. If acetaldehyde is

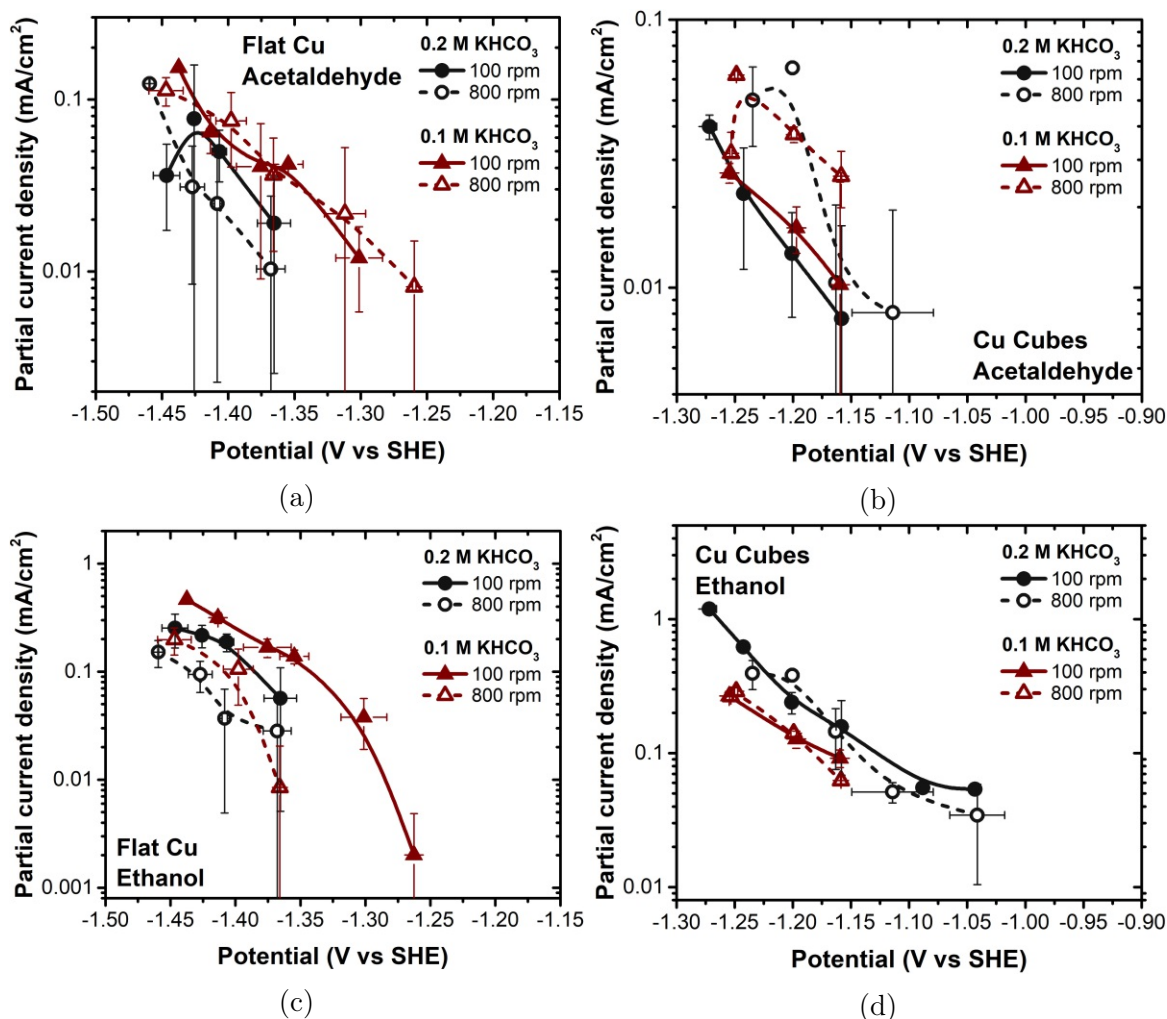


Figure 4.11: Partial CD of acetaldehyde for (a) polycrystalline copper (b) copper nanocubes and ethanol for (c) polycrystalline copper (d) copper nanocubes

indeed one of the intermediates of ethanol a decrease in the formation of this alcohol with shorter BLT could be expected. But again, the rotation speed should only affect the flux of species at the outermost electrode surface and only partially the entrance of the pores. Therefore, the enhancement of acetaldehyde should take mainly place there, while it is almost completely further reduced to ethanol in the pores due to the long retention time as it was already explained in chapter 4.4.

A similar behavior can be also seen from the experimental results for propionaldehyde and n-propanol where now also a slight decrease in the formation of the alcohol can be noted for 800 rpm when using the copper nanocubes as catalyst (Fig.A.5). To further outline this observations the ratio of aldehydes to alcohols are depicted for both catalysts in figure 4.12 where it can be learned that lower rotation speed and higher KHCO_3 are beneficial to drive the selectivity of the CO_2RR towards alcohols. Furthermore, it provides another evidence with direct experimental observations that

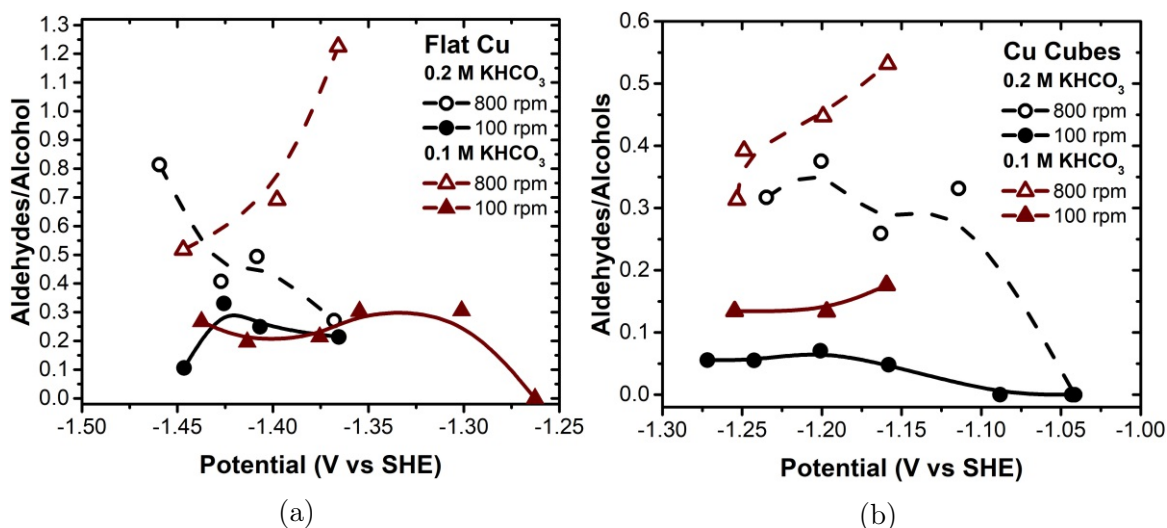


Figure 4.12: Ratio of aldehydes to alcohols for (a) polycrystalline copper (b) copper nanocubes

as already shown by Hori et al., aldehydes are the intermediates on the CO₂RR pathway to alcohols.

Remaining products

The partial CDs of the remaining products are illustrated in figure A.6 where most of them are already close to the detection limit of the applied quantification method (H-NMR). Therefore, only for ethylenglycol and acetate reliable statements can be made.

Ethylene glycol is showing the same dependence on the rotation speed and buffer concentration as ethanol and ethylene when using polycrystalline copper as the catalyst. In contrary, for the copper nanocubes no significant influence from both parameters could be observed which indicates that ethylene glycol since it is a C₂₊ product is mainly produced inside the pores.

The partial CD of acetate shows no significant dependence on neither the rotation speed nor the KHCO₃ concentration which makes it hard to say anything about how to change the selectivity towards this product.

Overall selectivity

Another important factor in the CO₂RR is the overall selectivity of the catalyst towards C₂₊ products and the capability to favor oxygenates over hydrocarbons since these chemical compounds have a higher market value.

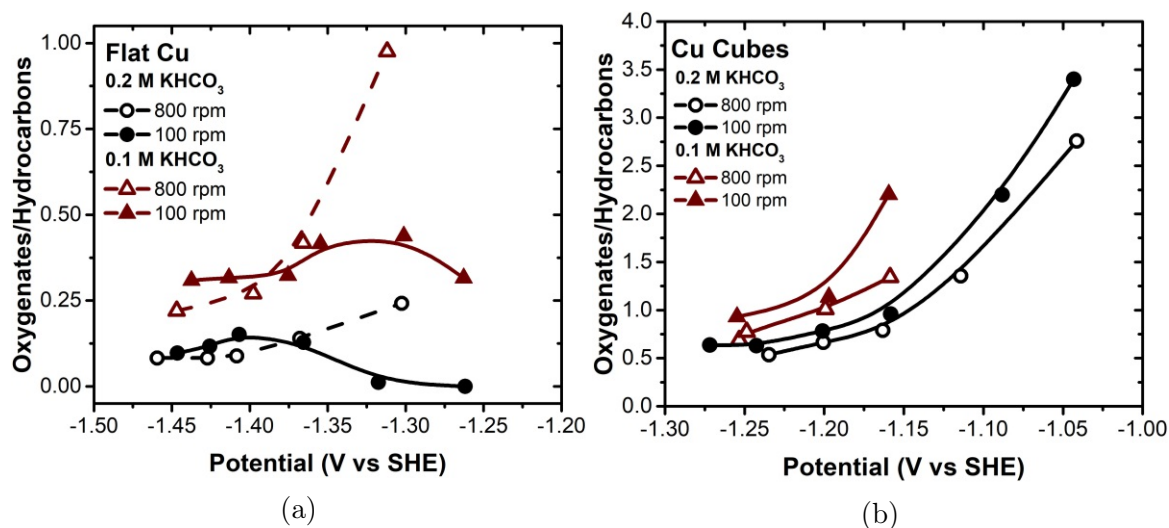


Figure 4.13: Ratio of $>2 e^-$ oxygenates to hydrocarbons for (a) polycrystalline copper (b) copper nanocubes

In the literature it was reported that a lower overpotential is favoring the production of oxygenates over hydrocarbons as it can be also seen for both of our tested catalysts (Fig.4.13). This should be due to the fact that the formation of hydrocarbons requires a more energy consuming C-O scission step and furthermore the surface coverage should shift from CO* to H* which is also more favorable for these higher hydrogenated species. Another important factor which has to be taken into account is the surface pH where a higher pH is favoring the formation of oxygenates over hydrocarbons. Hori et al. tried to explain the enhancement of oxygenates formation through higher pH by the possibility of a base-catalyzed reaction mechanism but a higher pH is also associated with a more negative onset potential for the HER which is resulting in a lower H* coverage at the same investigated potential. [37]

Comparing both catalysts, it can be seen that the copper cubes are exhibiting a higher ratio which is probably due to the investigation of a lower potential regime. Nevertheless, these results are showing that by using a nanostructured copper catalyst a desired ratio of oxygenates to hydrocarbons can be reached at a less energy consuming regime where on polycrystalline copper mainly the formation of hydrogen, CO and formate takes place.

Furthermore, a higher rotation speed is favoring the formation of hydrocarbons over oxygenates which is probably due to the higher flux of bicarbonate molecules to the electrode surface. Thereby, the surface pH is lowered and in addition KHCO₃ can serve as a proton donor to facilitate the hydrogenation to hydrocarbons.

Looking at the selectivity towards C₂₊ products on polycrystalline copper an enhancement can be achieved by using a lower buffer concentration and a lower rotation speed

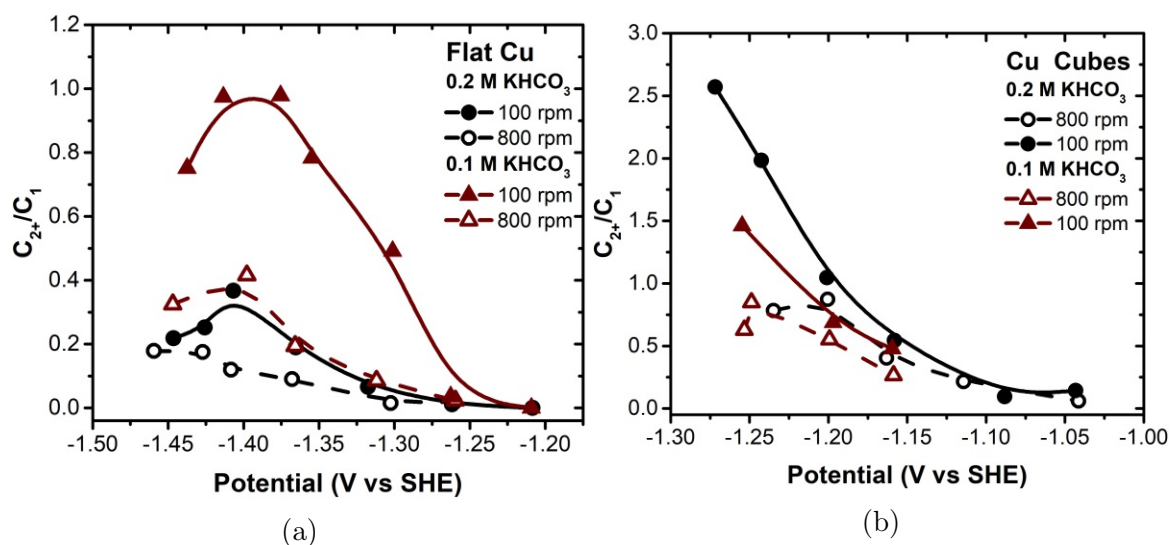


Figure 4.14: Ratio of C₂₊ to C₁ products for (a) polycrystalline copper (b) copper nanocubes

(Fig.4.14). This should be due to the fact that a higher pH near the electrode surface can be achieved and the retention time of intermediates undergoing C-C coupling can be prolonged. At more negative overpotential the electrochemical reduction towards methane is facilitated which is causing a shift of the selectivity back to C₁ products. In contrary, for the copper nanocubes higher buffer concentration is driving the selectivity towards C₂₊ products which is probably caused by the depletion of CO₂ inside the high alkaline pores as already discussed. Again higher rotation speed is favoring C₁ products even though the C-C coupling is mainly happening non influenced by the changing BLT inside the pores. In this case it is indebted by the higher flux of carbon monoxide away from the surface and the enhancement of formate formation with higher rotation speed as it can be seen from the total CD (Fig.4.5)

Nevertheless, it can be concluded that the copper nanocubes are presenting an active catalyst for the CO₂RR showing a high selectivity towards C-C coupling and C₂₊ oxygenates over hydrocarbons at low overpotential.

Chapter 5

CO₂ & NO₂⁻ Reduction

In this chapter of the thesis the preparation of the catalysts and results in the simultaneous electrochemical reduction of CO₂ and NO₂⁻ are going to be discussed. The catalysts were divided into three groups, namely the copper, titanium and titanium oxide group, and are going to be described separately. In the end, the CD towards ammonia for all the catalysts is going to be compared.

5.1 Copper Group

Copper was the first catalyst tested for its activity to produce urea. In previous studies it was shown that copper used as catalyst in a gas diffusion electrode setup can produce urea with a FE up to 37 % at -0.75 V vs SHE. [23]. Motivated by that we tested polycrystalline copper and copper nanocubes which are known for enhanced C-C coupling at different potentials.

Preparation of Catalyst

Both catalysts were prepared as already described in chapter 3.3.2. In contrast to the preparation of the copper nanocubes for the CO₂RR studies a polycrystalline copper foil was used as a substrate for the synthesis (Fig.5.1 b). The current during the redox cycling can be seen in Figure 5.1 (a) where a higher current was measured due to the higher surface area of the foil compared to the cylinder. The cyclic voltammogram is revealing the same shape which was already described in chapter 4.3 and also the color of the foil (Fig.5.1 c), caused by the nanostructured surface, is the same as for the copper nanocubes synthesized on the cylinder.

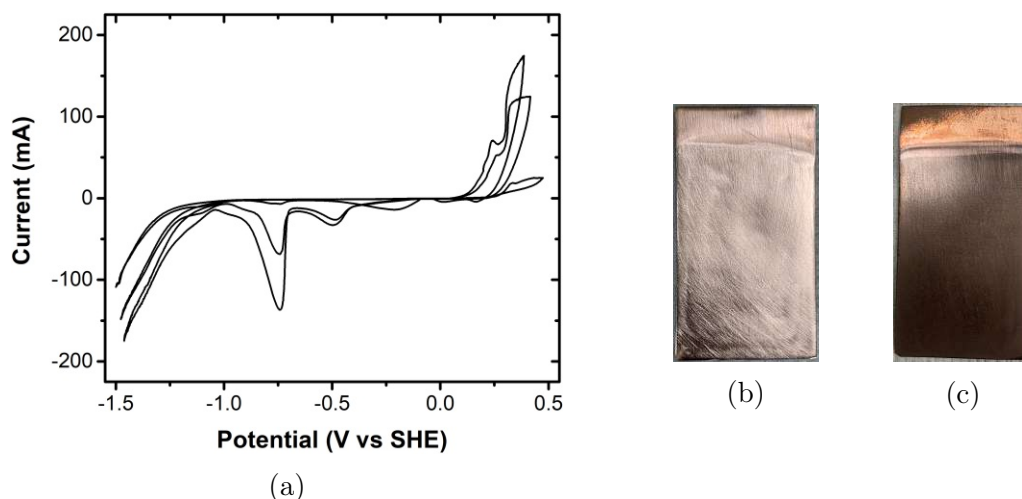


Figure 5.1: (a) Redox-Cycling of polycrystalline copper foil in 0.1 M KHCO_2 and 4 mM KCl for synthesis of copper nanocubes (b) polycrystalline copper (b) copper nanocubes

Results

In figure 5.2 the CD and FE for all the detected products catalyzed by polycrystalline copper (a) and copper nanocubes (b) are shown, whereby the products coming from the CO_2RR are plotted as one data point. For none of the performed experiments any molecules containing C-N bonds could be detected by H-NMR and also not urea by HPLC.

Comparing these results to those of Shibata et al. [23] where a high FE towards urea was achieved two reasons could serve as an explanation why we were not able to produce urea. Firstly, using gas diffusion electrodes provides the advantage of a facilitated transportation of CO_2 to the surface which is resulting in a higher surface coverage of CO_2RR intermediates. [38] Thereby, a favorable ratio of the surface coverage between CO-like and NH_3 -like intermediates could be reached which could be a necessary condition for the two coupling steps to synthesize urea. Secondly, copper was infiltrated into the gas diffusion electrode by a wet chemical approach followed by a heat treatment to activate the catalyst. This could result in the favoring of crystal facets and in a different surface morphology which could as well explain the high activity towards urea.

As can be seen in figure 5.2 by applying a more negative potential the selectivity of polycrystalline copper and copper nanocubes are shifting from ammonia towards hydrogen and CO_2RR products. At -0.95 V vs SHE about 35 % of the FE is missing for copper whereas for the copper nanocubes it is summing up to a 100 % for all the detected products. Intermediates on the electrochemical reduction pathway of

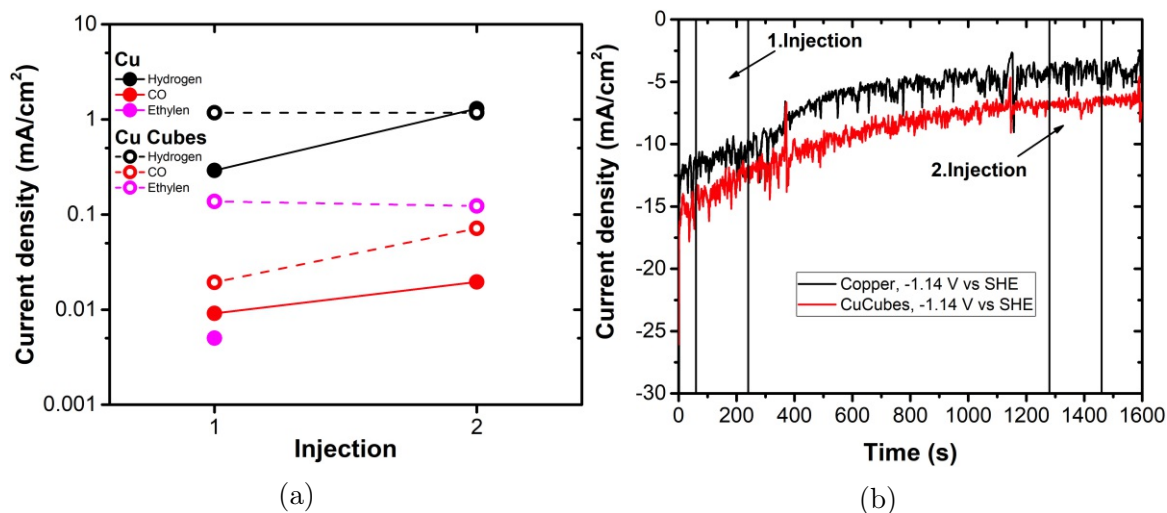


Figure 5.3: (a) Comparison of gaseous product's CDs for first and second GC injection for polycrystalline copper at -1.14 V vs SHE and copper nanocubes at -1.14 vs SHE (b) Chronoamperometry for polycrystalline copper at -1.14 V vs SHE (black line) and copper nanocubes at -1.14 vs SHE (red line)

CO^* . Therefore, a higher CD towards hydrogen and CO is not surprising. Secondly, since over time the total CD is decreasing the production of hydroxyl ions is also decreasing which is leading to a lower pH near the surface. From the CO_2RR data, discussed in chapter 4 we could learn that a higher pH is favoring the production of ethylene, which could explain the decreasing partial CD of this C_2 product over time.

5.2 Titanium Group

For the next group, titanium and electrochemically deposited copper on titanium were investigated for the production of urea. The deposition process was performed as described by Mandke et al. [39], where they were able to grow spherical nanoparticles with an average particle size of 750 nm on fluorine doped tin oxide. Thereby, the goal was to tune the selectivity of copper towards C-N coupling by changing the surface morphology and compare the experimental results to titanium.

Preparation of Catalyst

In figure 5.4 (a) the CD during the electrochemically deposition of copper on titanium is illustrated. After the deposition process it was clearly visible that a thin layer of copper was grown on the titanium foil (Fig.5.4 b).

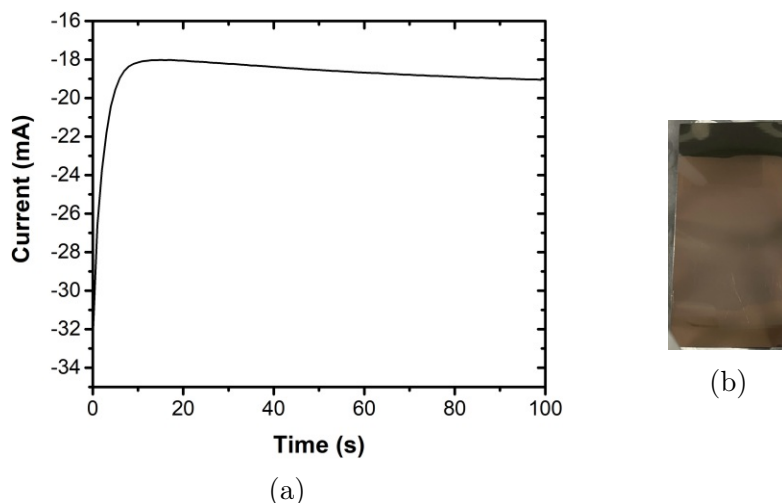


Figure 5.4: (a) Electrodeposition of copper on pre-cleaned titanium foil at -1.5 V vs carbon foil from 140 mL of 0.1 M CuSO_4 and 1 M citric acid for 100 seconds (b) copper deposited on titanium

Results

The FE and CD for all the detected products are plotted in figure 5.5, where again the CO_2RR products are summarized as one point. Neither for titanium nor for the deposited copper any molecules containing carbon nitrogen bonds could be detected by the used analytical methods (H-NMR, HPLC).

For titanium at both tested potentials some FE is missing which could be again explained by possible intermediates of the nitrite to ammonia reduction pathway which are not detectable by our applied analytical methods. Furthermore, for more

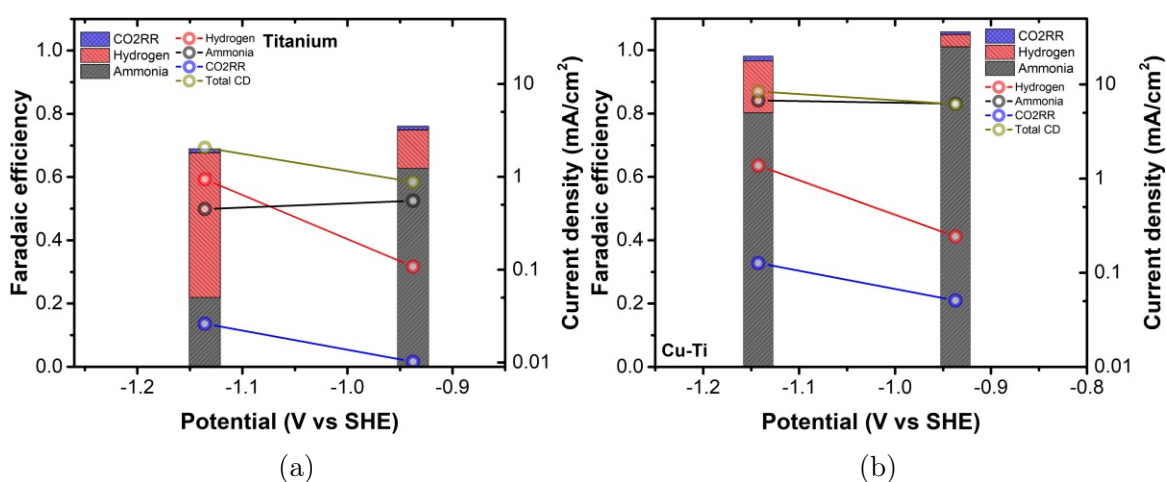


Figure 5.5: FE and CD of products synthesized during the simultaneous electrochemical reduction of CO_2 and NO_2^- for (a) titanium foil (b) copper deposited on titanium tested at different potentials vs SHE

negative potential a selectivity change towards hydrogen and a decreasing partial CD for ammonia can be observed.

For the deposited copper on titanium the FE is summing up to around 100 % and the major product is ammonia for both tested potentials. These results are very similar to those observed at the same potentials for the copper nanocubes, which indicates that both catalysts could reveal the same active sites towards the reduction of nitrite to ammonia. Nevertheless, only carbon monoxide, formate and acetate but no C-C coupling products were observed for the deposited copper, whereas the copper nanocubes were still catalyzing products as ethanol and ethylene.

5.3 Titanium Oxide Group

In previous studies it was shown that P25 TiO_2 nanoparticles [25] and TiO_2 nanotubes [26] are able to catalyze urea with a FE of 40 and 43 % at a potential of -0.52 and -0.4 V vs RHE. Therefore, two different electrochemically anodized grown titanium oxides were tested for their activity to synthesis molecules containing carbon-nitrogen bonds during the simultaneous reduction of CO_2 and NO_2^- .

Preparation of Catalyst

Two titanium oxide layers were grown on a pre-cleaned titanium foil as already described in chapter 3.3.2. Thereby, two different electrolytes, namely 0.1 M perchloric acid and 0.4 M ammonium chloride (pH 1.5) were tested at 20 and 18 V since under these conditions the successful growth of titanium oxide nanotubes was reported. [40] [41] In figure 5.6 the measured current for both methods are plotted and the surface color of the titanium oxide layers after the annealing treatment are shown. During the electrochemically anodization in 0.1 M perchloric acid a higher oxidative current and a lighter bluish surface color for the titanium oxide layer could be observed. From the higher current a thicker oxide layer can be expected, which in turn can explain the difference in the surface color. Nevertheless, no SEM images were made of both samples, thereby a successful growth of titanium oxide nanotubes couldn't be confirmed and has to be part of future work.

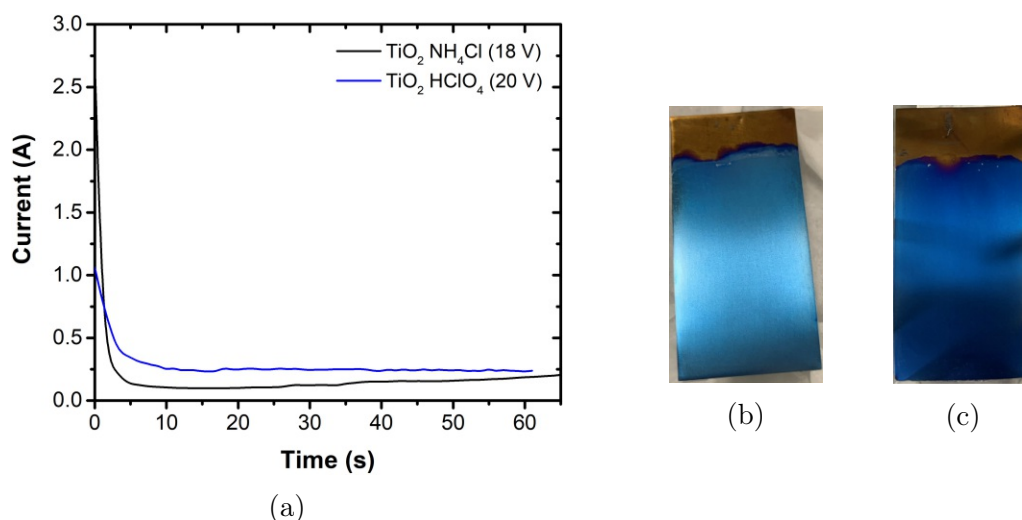


Figure 5.6: (a) Anodic growth of titanium oxide in 0.1 M HClO_4 at 20 V vs Pt foil (blue line) and in 0.4 M NH_4Cl (pH 1.5) at 18 V vs Pt foil (black line) (b) $\text{TiO}_2 \text{ HClO}_4$ (c) $\text{TiO}_2 \text{ NH}_4\text{Cl}$

Results

The results for both titanium oxide layers can be seen in figure 5.7, where the FE and CD is illustrated for the tested potentials. For each investigated condition the main detected product is ammonia and only for the most negative potential hydrogen and trace amounts of formate were quantified. Again, no products containing carbon-nitrogen bonds were detected by the applied analytical methods (H-NMR, HPLC). For both catalysts an decrease in the total FE with increasing potential can be observed, which can be explained again by intermediates, as hydroxyl amine, of the

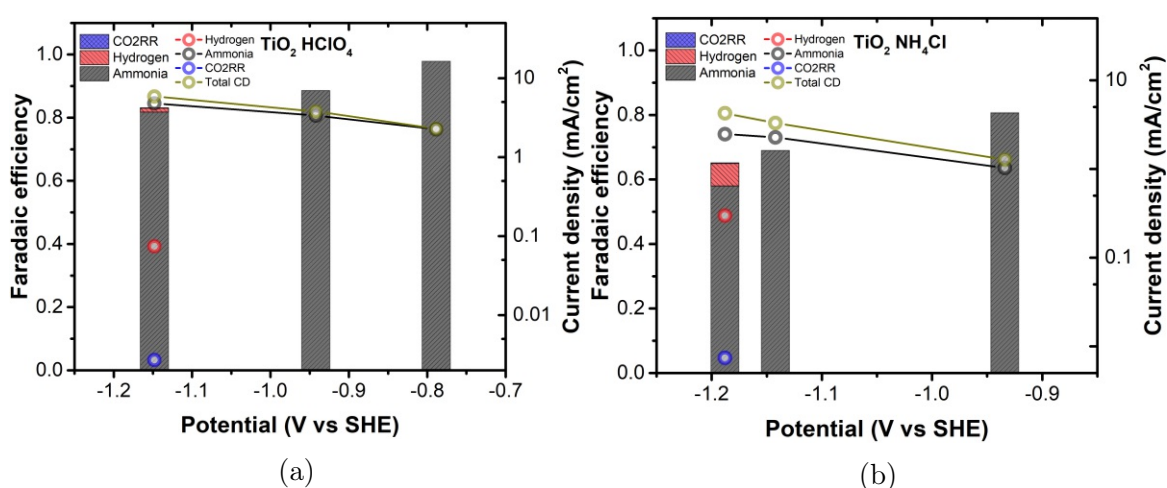


Figure 5.7: FE and CD for products synthesized during the simultaneous electrochemical reduction of CO_2 and NO_2^- for (a) $\text{TiO}_2 \text{ HClO}_4$ (b) $\text{TiO}_2 \text{ NH}_4\text{Cl}$ tested at different potentials vs SHE

nitrite to ammonia reduction pathway which can not be detected by the used analytical methods in this study. Furthermore, the titanium oxide, grown in 0.1 M perchloric acid is revealing a higher activity towards ammonia, where future studies should be done to explain the difference between both titanium oxide layers.

5.4 Comparison of CD and FE towards ammonia

In this section the CD and selectivity towards ammonia for each tested catalyst is going to be compared. As can be seen in figure 5.8, the copper nanocubes are showing the highest activity and FE towards ammonia where nearly same good results were achieved by the electrochemically deposited copper on titanium. From that it can be concluded, that a high surface area modification of copper can reduce nitrite to ammonia with a high activity and selectivity even while bubbling CO_2 in the electrolyte. The high selectivity compared to polycrystalline copper can be explained by the porous structure of both catalysts which gives the intermediates of the nitrite to ammonia reduction pathway a longer retention time inside the porous structure thereby increasing the likelihood of a re-absorption and further reduction to ammonia. Moreover, it can be seen that the titanium oxide layer grown in 0.1 M perchloric acid is revealing a higher CD and FE towards ammonia than the one grown in 0.4 M ammonium chloride. Again, this experimental observation could be explained by a higher surface area and more porous structure of the first titanium oxide layer, since from the synthesis process a thicker oxide layer can be expected.

Overall, these experimental results are suggesting that a high surface area and nano

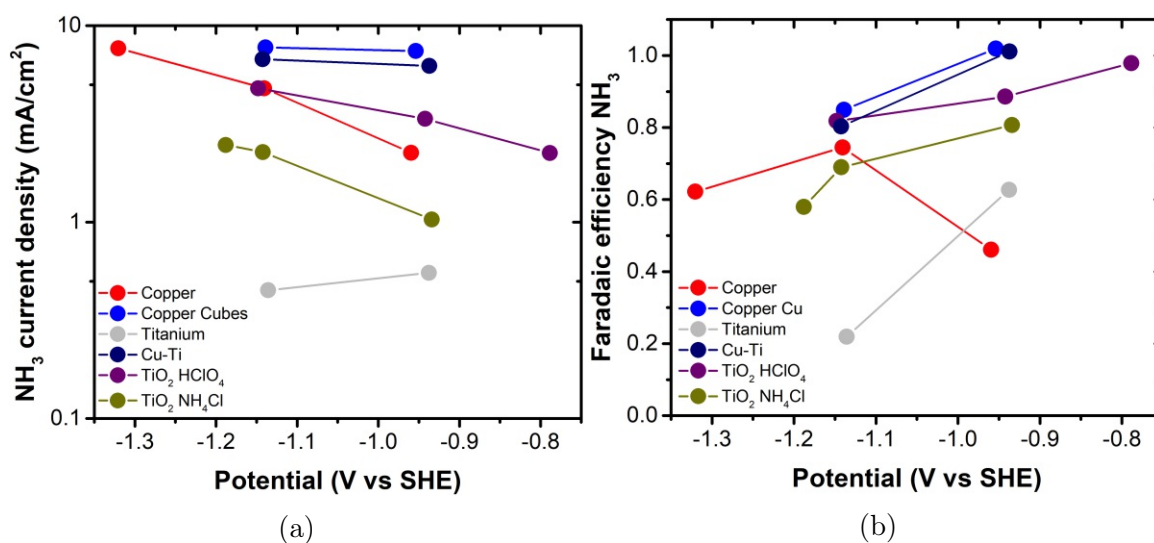


Figure 5.8: Comparison of CD (a) and FE (b) of ammonia for all the catalysts tested in the simultaneous electrochemical reduction of CO_2 and NO_2^-

porous catalyst is very beneficial for a high activity of the reduction of nitrite towards ammonia, where nano-structured copper should be included in future investigations.

Chapter 6

Conclusion & Outlook

6.1 Summary - CO₂RR

The first part of the thesis was focused on the investigation of copper nanocubes, a nano porous copper catalyst, which is able to perform C-C coupling with a high selectivity. Especially, the high ratio of ethylene over methane made this catalyst famous where in previous studies this finding was explained by the high amount of (100)-crystal facets on the surface. [16] [17]

In this study we were able to suggest a new theory by conducting experiments with our state of the art gas-tight rotation cell and comparing these observations to the results gathered on polycrystalline copper by Rüscher [1] using the same setup. By rotating the electrode we were able to systematically control the mass transport and thereby we could see that the partial CD of C₂₊ products is not significantly affected by the changing BLT when using copper nanocubes as a catalyst. As an explanation we hypothesize that inside the porous system, which is not influenced by the diffusive flux near the outer electrode surface, most of the C-C coupling is occurring. Inside the pores a high pH value is securing perfect conditions for the formation of C₂₊ products and a suppression for highly hydrogenated C₁ species as methane. In addition, the high retention time of intermediates inside the pores is increasing the likelihood of re absorption and reduction to further reduced products. Furthermore, we were also able to provide direct experimental evidence that aldehydes are the main intermediates on the CO₂RR pathway to alcohols.

6.2 Outlook - CO₂RR

6.2.1 New Cell Design

For future experiments a new gas-tight rotation cell was designed to overcome drawbacks of the old cell. The major limitation was the high resistance between the working and the counter electrode due to the long distance and small cross section of the ion bridge. Therefore, the new cell is a combination of the old cell and the compression cell which was designed by Kuhl et al. [14], where the counter compartment is now connected to the working side as it is known for "sandwich-type" cells. Thereby, the cross section of the membrane is wider and the distance between the working and counter electrode is shorter which in addition solves the problem of bubble formation, as it was the case for the previous ion bridge. With this optimization CDs up to 150 mA·cm⁻² can be reached which is closer to the desired current in future industrial applications.

Furthermore, a pocket underneath the working side was included where a cooling block can be placed. Through that the temperature of the electrolyte can now be lowered by using a thermostat.

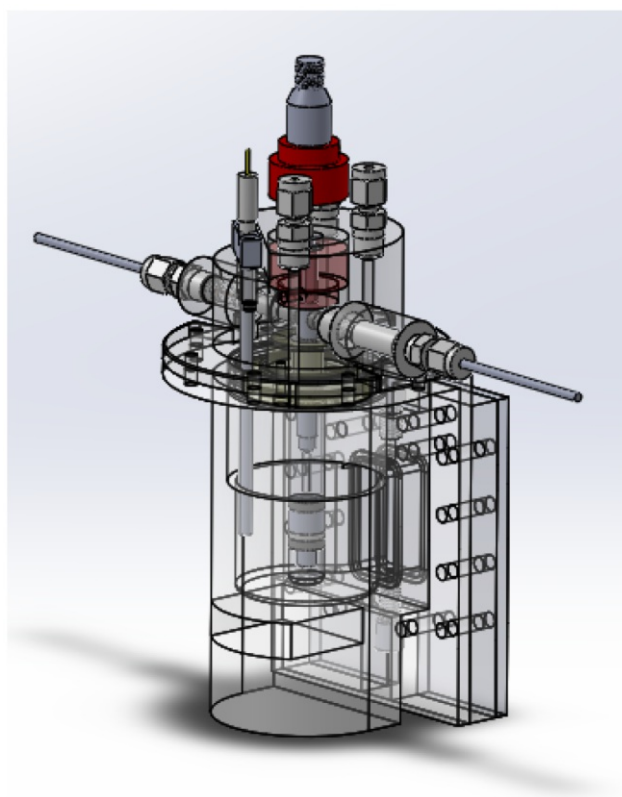


Figure 6.1: Design of the new gas-tight rotation cell [1]

6.2.2 Experimental

With these studies and previous investigations by Rüscher [1] it was shown that by controlling the mass transport valuable new insights about the occurring mechanism and influences of the catalyst's surface structure in the CO₂RR can be gained.

In the future a new parameter can be included since the new rotation cell setup allows now to lower the temperature of the electrolyte. It is understood that by lowering the temperature a higher solubility of CO₂ can be reached. Hori et.al was the first who studied the CO₂RR on copper at different temperature and he could observe a selectivity shift towards methane and a suppression of the HER by lowering the temperature. [42] But so far it is not well understood how temperature is affecting the electrochemical reduction of CO₂ and therefore future experiments should be done with the new rotation cell setup to gain new valuable knowledge by controlling the mass transport.

Another goal for the future should be to gain a better understanding of the reaction pathway in the CO₂RR. Therefore, experiments should be performed with the same reactions conditions while using a known intermediate as the starting material instead of CO₂. From the experimental results on polycrystalline copper and reports in the literature CO is well known as one of the key intermediates and is thereby providing a good starting point for first investigations.

6.3 CO₂ & NO₂⁻ Reduction - Summary & Outlook

The second topic was focused on the simultaneously electrochemical reduction of CO₂ and NO₂⁻ with urea as the target product. This was motivated by previous reports in the literature where a high FE towards urea was yielded. [23] [25] [26]

In the course of this work three different groups of catalysts were tested, namely the copper, titanium, and titanium oxide group. For none of the tested materials urea was detected inside the working electrolyte after performing the electrolysis. Furthermore, also no product containing a C-N bond could be detected by means of H-NMR. Nevertheless, with the experimental results it was observed that a nonporous catalyst is revealing a high FE when reducing nitrite to ammonia where the copper nanocubes were exhibiting the highest activity and selectivity.

In the future new catalysts have to be designed and tested towards their activity to produce urea out of CO₂ and NO₂⁻. A new starting point could be the investigation of more transition metals based on the results gathered by Shibata et al. [24] After finding an active catalyst the material should be adopted for the gas tight RCE setup to investigate the electrocatalytic process under controlled mass transport conditions

to learn more about the kinetics of the occurring mechanism.

Bibliography

- [1] Rüscher Martina. Mass transport effects on product distribution during electrochemical CO₂ reduction in a custom-designed rotating cylindrical electrode cell. 2021.
- [2] Adam R Martin and Sean C Thomas. A reassessment of carbon content in tropical trees. *PloS one*, 6(8):e23533, 2011.
- [3] Holli Riebeek. Global warming: Feature articles. 2010.
- [4] Masaki Yoshio, Ralph J Brodd, and Akiya Kozawa. *Lithium-ion batteries*, volume 1. Springer, 2009.
- [5] Manish Kumar Singla, Parag Nijhawan, and Amandeep Singh Oberoi. Hydrogen fuel and fuel cell technology for 61a cleaner future: 61a review. *Environmental Science and Pollution Research*, pages 1–20, 2021.
- [6] L Fiamelda et al. Analysis of water and electricity consumption of urea fertilizer industry: case study pt. x. In *IOP Conference Series: Earth and Environmental Science*, volume 472, page 012034. IOP Publishing, 2020.
- [7] Masami Shibata, Kohji Yoshida, and Nagakazu Furuya. Electrochemical synthesis of urea at gas-diffusion electrodes. 1. simultaneous reduction of carbon dioxide and nitrite ions at Zn catalysts; gas kakusan denkyoku wo mochiita nyoso denkai gosei. 1. aen shokubaijo deno nisanka tanso to ashosan ion no doji kangen. *Denki Kagaku Oyobi Kogyo Butsuri Kagaku (Electrochemistry and Industrial Physical Chemistry)*, 64, 1996.
- [8] Kari Pirkanniemi and Mika Sillanpää. Heterogeneous water phase catalysis as an environmental application: a review. *Chemosphere*, 48(10):1047–1060, 2002.
- [9] Zengcai Liu, Richard I Masel, Qingmei Chen, Robert Kutz, Hongzhou Yang, Krzysztof Lewinski, Marina Kaplun, Sean Luopa, and Dale R Lutz. Electrochemical generation of syngas from water and carbon dioxide at industrially important rates. *Journal of CO₂ Utilization*, 15:50–56, 2016.

- [10] Zengcai Liu, Hongzhou Yang, Robert Kutz, and Richard I Masel. Co₂ electrolysis to co and o₂ at high selectivity, stability and efficiency using sustainion membranes. *Journal of The Electrochemical Society*, 165(15):J3371, 2018.
- [11] Juan Herranz, Alexandra Patru, Emiliana Fabbri, and Thomas J Schmidt. Co-electrolysis of co₂ and h₂o: from electrode reactions to cell level development. *Current Opinion in Electrochemistry*, 2020.
- [12] Yoshio Hori, Katsuhei Kikuchi, Akira Murata, and Shin Suzuki. Production of methane and ethylene in electrochemical reduction of carbon dioxide at copper electrode in aqueous hydrogencarbonate solution. *Chemistry Letters*, 15(6):897–898, 1986.
- [13] Yoshio Hori, Akira Murata, and Ryutaro Takahashi. Formation of hydrocarbons in the electrochemical reduction of carbon dioxide at a copper electrode in aqueous solution. *Journal of the Chemical Society, Faraday Transactions 1: Physical Chemistry in Condensed Phases*, 85(8):2309–2326, 1989.
- [14] Kendra P Kuhl, Etosha R Cave, David N Abram, and Thomas F Jaramillo. New insights into the electrochemical reduction of carbon dioxide on metallic copper surfaces. *Energy & Environmental Science*, 5(5):7050–7059, 2012.
- [15] Stephanie Nitopi, Erlend Bertheussen, Soren B Scott, Xinyan Liu, Albert K Engstfeld, Sebastian Horch, Brian Seger, Ifan EL Stephens, Karen Chan, Christopher Hahn, et al. Progress and perspectives of electrochemical co₂ reduction on copper in aqueous electrolyte. *Chemical reviews*, 119(12):7610–7672, 2019.
- [16] F Sloan Roberts, Kendra P Kuhl, and Anders Nilsson. High selectivity for ethylene from carbon dioxide reduction over copper nanocube electrocatalysts. *Angewandte Chemie*, 127(17):5268–5271, 2015.
- [17] F Sloan Roberts, Kendra P Kuhl, and Anders Nilsson. Electroreduction of carbon monoxide over a copper nanocube catalyst: surface structure and ph dependence on selectivity. *ChemCatChem*, 8(6):1119–1124, 2016.
- [18] André Eilert, F Sloan Roberts, Daniel Friebel, and Anders Nilsson. Formation of copper catalysts for co₂ reduction with high ethylene/methane product ratio investigated with in situ x-ray absorption spectroscopy. *The journal of physical chemistry letters*, 7(8):1466–1470, 2016.

- [19] Lei Wang, Stephanie A Nitopi, Erlend Bertheussen, Marat Orazov, Carlos G Morales-Guio, Xinyan Liu, Drew C Higgins, Karen Chan, Jens K Nørskov, Christopher Hahn, et al. Electrochemical carbon monoxide reduction on polycrystalline copper: Effects of potential, pressure, and ph on selectivity toward multicarbon and oxygenated products. *Acs Catalysis*, 8(8):7445–7454, 2018.
- [20] DR Gabe. The rotating cylinder electrode. *Journal of Applied Electrochemistry*, 4(2):91–108, 1974.
- [21] J Robert Selman and Charles W Tobias. Mass-transfer measurements by the limiting-current technique. In *Advances in chemical engineering*, volume 10, pages 211–318. Elsevier, 1978.
- [22] WT Mook, MH Chakrabarti, MK Aroua, GMA Khan, BS Ali, MS Islam, and MA Abu Hassan. Removal of total ammonia nitrogen (tan), nitrate and total organic carbon (toc) from aquaculture wastewater using electrochemical technology: a review. *Desalination*, 285:1–13, 2012.
- [23] Masami Shibata, Kohji Yoshida, and Nagakazu Furuya. Electrochemical synthesis of urea at gas-diffusion electrodes: Part ii. simultaneous reduction of carbon dioxide and nitrite ions at cu, ag and au catalysts, 1998.
- [24] Masami Shibata, Kohji Yoshida, and Nagakazu Furuya. Electrochemical synthesis of urea at gas-diffusion electrodes: Part iii. simultaneous reduction of carbon dioxide and nitrite ions with various metal catalysts. *Journal of the Electrochemical Society*, 145(2):595, 1998.
- [25] Duraisamy Saravanakumar, Jieun Song, Sunhye Lee, Nam Hwi Hur, and Woonup Shin. Electrocatalytic conversion of carbon dioxide and nitrate ions to urea by a titania–nafion composite electrode. *ChemSusChem*, 10(20):3999–4003, 2017.
- [26] Na Cao, Yueli Quan, Anxiang Guan, Chao Yang, Yali Ji, Lijuan Zhang, and Gengfeng Zheng. Oxygen vacancies enhanced cooperative electrocatalytic reduction of carbon dioxide and nitrite ions to urea. *Journal of Colloid and Interface Science*, 577:109–114, 2020.
- [27] Suho Jung, Ruud Kortlever, Ryan JR Jones, Michael F Lichterman, Theodor Agapie, Charles CL McCrory, and Jonas C Peters. Gastight hydrodynamic electrochemistry: design for a hermetically sealed rotating disk electrode cell. *Analytical chemistry*, 89(1):581–585, 2017.

- [28] F Sloan Roberts, Kendra P Kuhl, and Anders Nilsson. High selectivity for ethylene from carbon dioxide reduction over copper nanocube electrocatalysts. *Angewandte Chemie*, 127(17):5268–5271, 2015.
- [29] Na Cao, Yueli Quan, Anxiang Guan, Chao Yang, Yali Ji, Lijuan Zhang, and Gengfeng Zheng. Oxygen vacancies enhanced cooperative electrocatalytic reduction of carbon dioxide and nitrite ions to urea. *Journal of Colloid and Interface Science*, 577:109–114, 2020.
- [30] Narges Fathy Fahim, Tohru Sekino, Magdi Farouk Morks, and Takafumi Kusunose. Electrochemical growth of vertically-oriented high aspect ratio titania nanotubes by rapid anodization in fluoride-free media. *Journal of nanoscience and nanotechnology*, 9(3):1803–1818, 2009.
- [31] C Richter, E Panaitescu, R Willey, and L Menon. Titania nanotubes prepared by anodization in fluorine-free acids. *Journal of materials research*, 22(6):1624–1631, 2007.
- [32] Shona Clark, Paul S Francis, Xavier A Conlan, and Neil W Barnett. Determination of urea using high-performance liquid chromatography with fluorescence detection after automated derivatisation with xanthinol. *Journal of Chromatography A*, 1161(1-2):207–213, 2007.
- [33] Yoshio Hori, Ryutaro Takahashi, Yuzuru Yoshinami, and Akira Murata. Electrochemical reduction of co at a copper electrode. *The Journal of Physical Chemistry B*, 101(36):7075–7081, 1997.
- [34] Yoshio Hori, Akira Murata, and Ryutaro Takahashi. Formation of hydrocarbons in the electrochemical reduction of carbon dioxide at a copper electrode in aqueous solution. *Journal of the Chemical Society, Faraday Transactions 1: Physical Chemistry in Condensed Phases*, 85(8):2309–2326, 1989.
- [35] Andrew A Peterson, Frank Abild-Pedersen, Felix Studt, Jan Rossmeisl, and Jens K Nørskov. How copper catalyzes the electroreduction of carbon dioxide into hydrocarbon fuels. *Energy & Environmental Science*, 3(9):1311–1315, 2010.
- [36] Yoshio Hori, Ryutaro Takahashi, Yuzuru Yoshinami, and Akira Murata. Electrochemical reduction of co at a copper electrode. *The Journal of Physical Chemistry B*, 101(36):7075–7081, 1997.
- [37] Lei Wang, Stephanie A Nitopi, Erlend Bertheussen, Marat Orazov, Carlos G Morales-Guio, Xinyan Liu, Drew C Higgins, Karen Chan, Jens K Nørskov,

- Christopher Hahn, et al. Electrochemical carbon monoxide reduction on polycrystalline copper: Effects of potential, pressure, and pH on selectivity toward multicarbon and oxygenated products. *Acs Catalysis*, 8(8):7445–7454, 2018.
- [38] Drew Higgins, Christopher Hahn, Chengxiang Xiang, Thomas F Jaramillo, and Adam Z Weber. Gas-diffusion electrodes for carbon dioxide reduction: a new paradigm. *ACS Energy Letters*, 4(1):317–324, 2018.
- [39] Mohanrao V Mandke and Habib M Pathan. Electrochemical growth of copper nanoparticles: structural and optical properties. *Journal of Electroanalytical Chemistry*, 686:19–24, 2012.
- [40] Narges Fathy Fahim, Tohru Sekino, Magdi Farouk Morks, and Takafumi Kusunose. Electrochemical growth of vertically-oriented high aspect ratio titania nanotubes by rapid anodization in fluoride-free media. *Journal of nanoscience and nanotechnology*, 9(3):1803–1818, 2009.
- [41] C Richter, E Panaitescu, R Willey, and L Menon. Titania nanotubes prepared by anodization in fluorine-free acids. *Journal of materials research*, 22(6):1624–1631, 2007.
- [42] Yoshio Hori, Akira Murata, and Ryutaro Takahashi. Formation of hydrocarbons in the electrochemical reduction of carbon dioxide at a copper electrode in aqueous solution. *Journal of the Chemical Society, Faraday Transactions 1: Physical Chemistry in Condensed Phases*, 85(8):2309–2326, 1989.

Appendix

Calibration

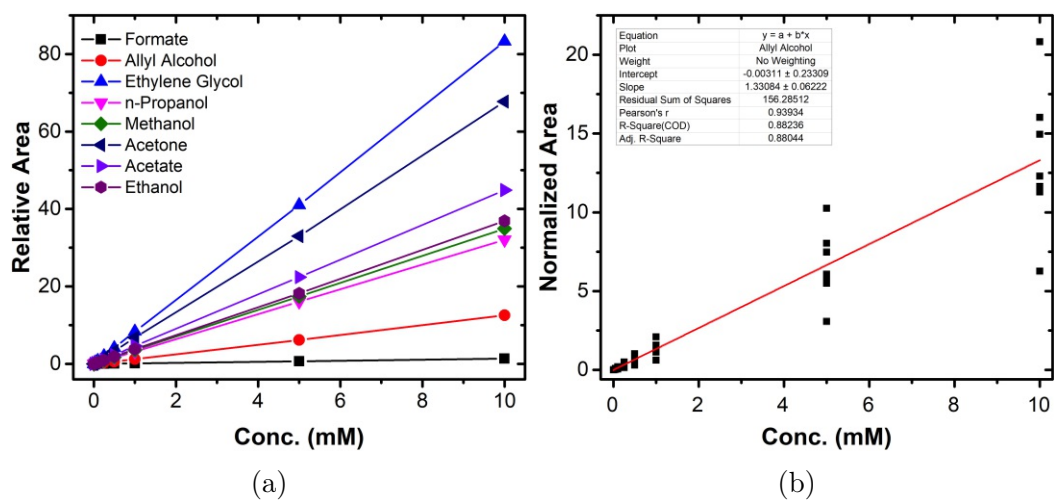


Figure A.1: Calibration curves for H-NMR (a) relative area (b) normalized area

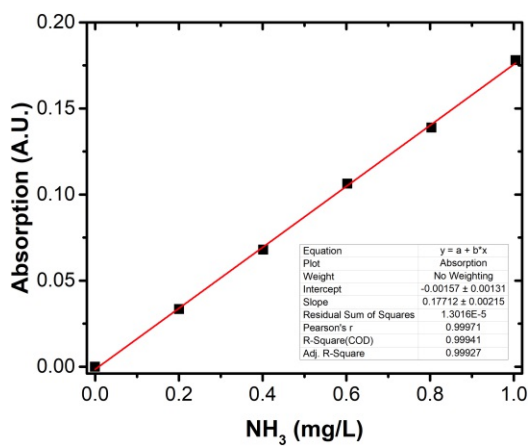


Figure A.2: Calibration curve for ammonia quantification (salicylic acid method)

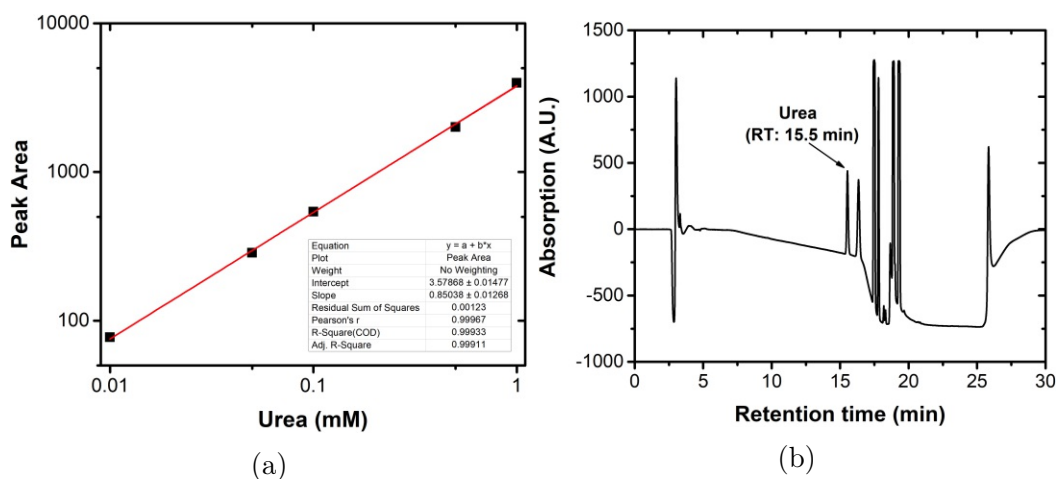


Figure A.3: (a) Calibration curves for urea (b) chromatogram for 1 mM urea standard

Table A.1: Results of calibration for GC

Gas	Content (ppm)	Peak Area	Retention Time (min)
Hydrogen	1000	23.5666	0.92
Methane	1016	6470.1	2.83
CO	1025	6154.7	4.30
Ethylene	1000	12758	7.53
Ethane	1007	12841	8.083

Additional Data

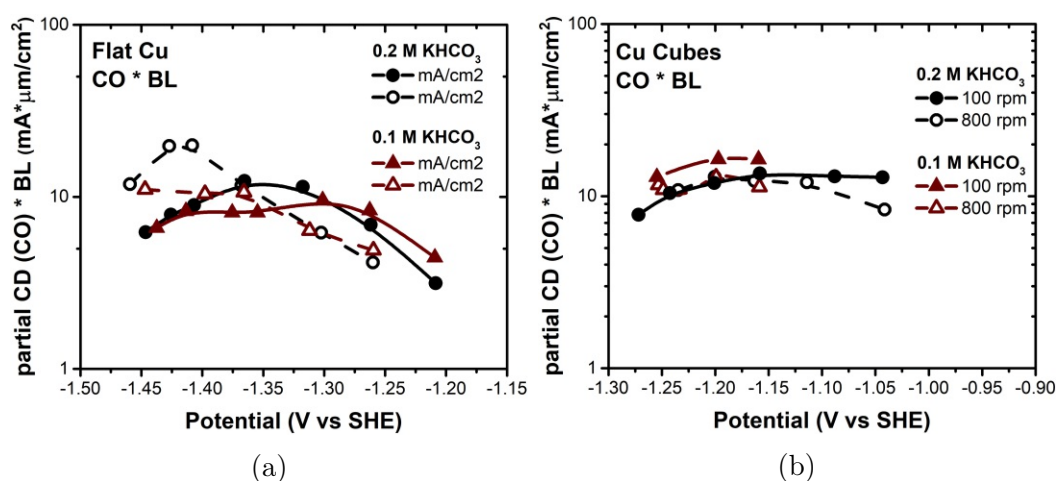


Figure A.4: Partial CD of CO normalized with BLT (a) polycrystalline copper (b) copper nanocubes

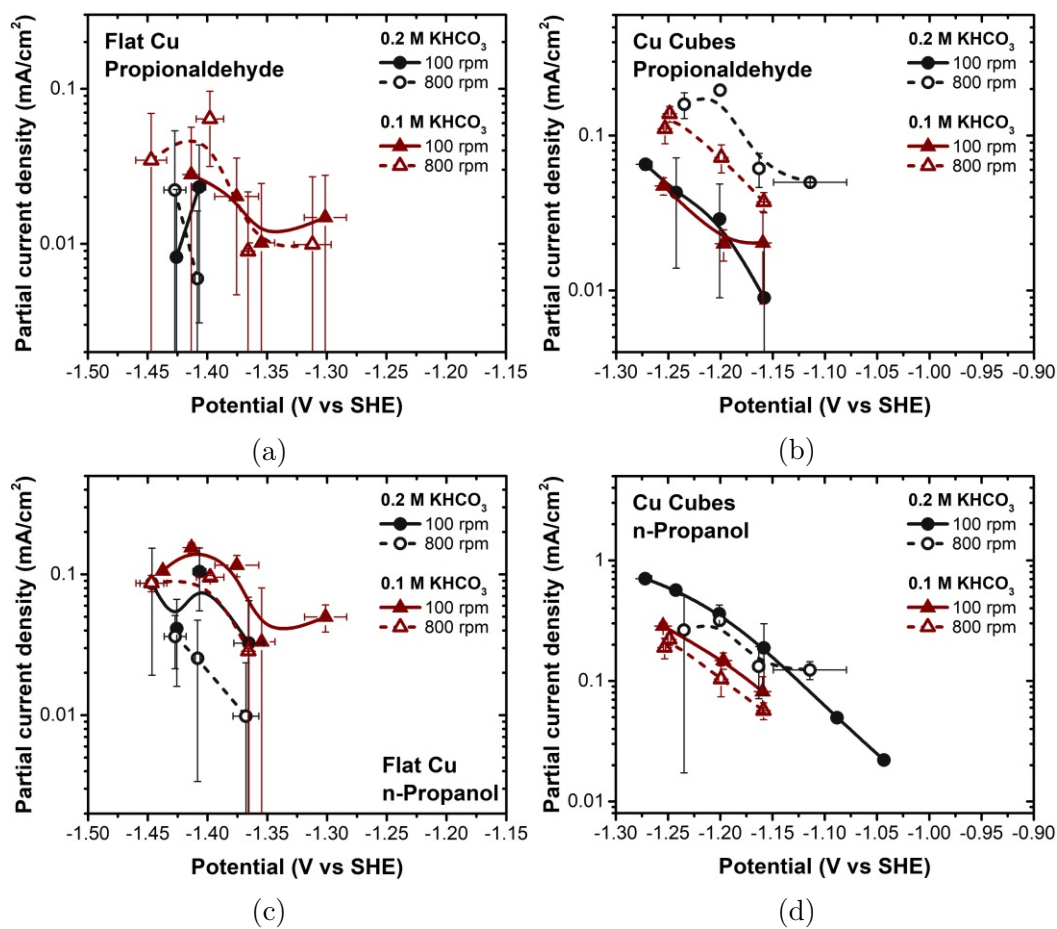


Figure A.5: Partial CD of propionaldehyde for (a) polycrystalline copper (b) copper nanocubes and n-propanol for (c) polycrystalline copper (d) copper nanocubes

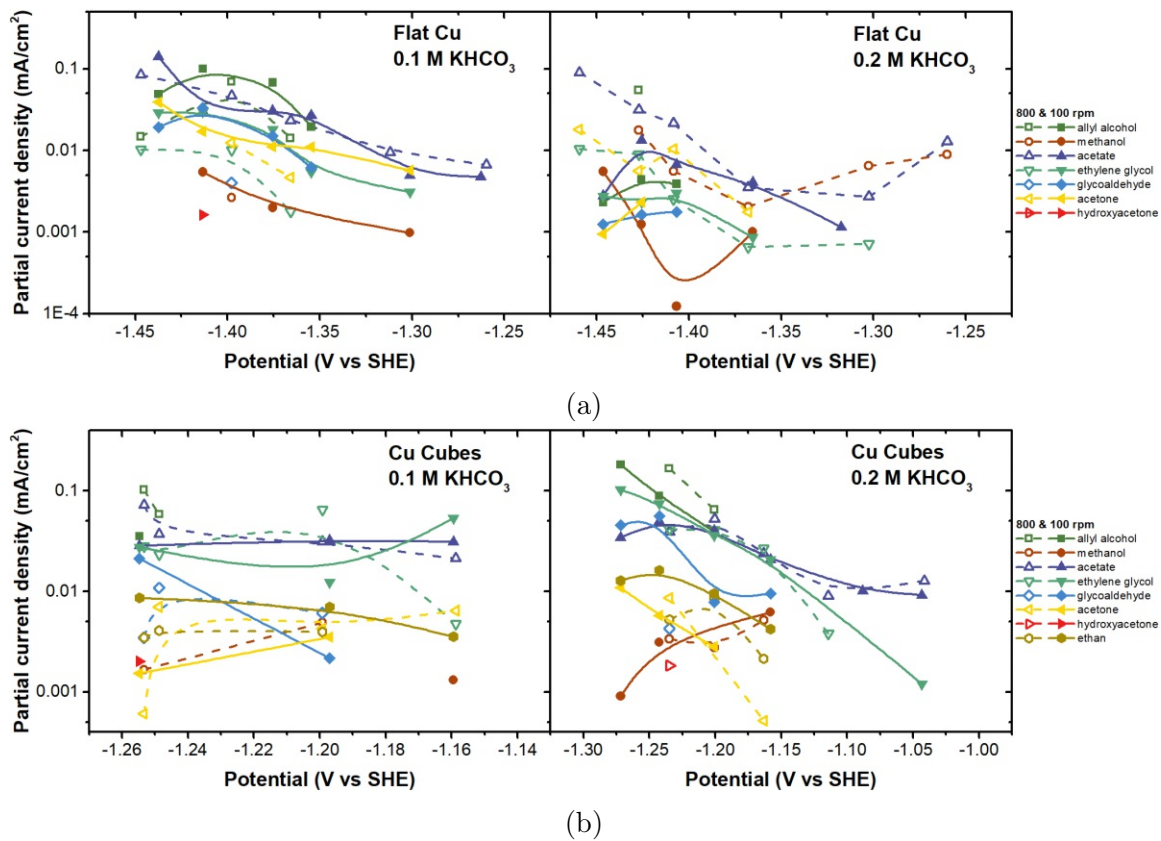


Figure A.6: Partial CD of remaining products (a) polycrystalline copper (b) copper nanocubes